

Systems Engineering and Project Management

MUSE 2020-2021

Concurrent Engineering: MARTINLARA PDR

Author:

María ALONSO ÁLVAREZ
Andrea BRAVO ASIÁN
Daniel DEL RÍO VELILLA
Laura GARCÍA MORENO
Rafael LUQUE LÓPEZ
Diego MATAIX CABALLERO
Marina MERCHÁN BRAVO
Siro MUELA MÁRQUEZ
Daniel NAVAJAS ORTEGA
María Elena PIQUERAS CARREÑO
Javier VEGA MATEOS
Pablo ZAPATERO MONTAÑA

Professors:

Jose Miguel ÁLVAREZ
Sergio MARÍN
Elena ROIBÁS



Contents

1	Introduction	7
2	Applicable and reference documents	8
3	Mission overview, requirements flow-down	11
4	Subsystem analysis and design	13
4.1	Mission Analysis	13
4.1.1	Introduction	13
4.1.2	Orbit analysis	13
4.1.3	Mission duration and access study	15
4.1.4	Results	17
4.1.5	Measurements Modes	18
4.2	Structure subsystem	18
4.2.1	Satellite Dispenser	18
4.2.2	Primary structure	20
4.2.3	Manufactured components	21
4.2.4	Deployable solar panel	23
4.2.5	Subsystem distribution	23
4.2.6	Final design	24
4.3	Thermal Control Subsystem	25
4.3.1	Requirements	25
4.3.2	Preliminary model	26
4.3.3	Discussion of results	29
4.4	Attitude Determination and Control Subsystem	29
4.4.1	Disturbance sizing	30
4.4.2	Spacecraft control selection	31
4.4.3	ADCS heritage designs	31
4.4.4	Trade-off analysis	32
4.4.5	ADCS components	33
4.4.6	ADCS Mission Operation Modes	34
4.5	Command and Data Handling	35
4.6	Communication Subsystem	36
4.6.1	Preliminary Link Design	36
4.6.2	Ground Station	36
4.6.3	Satellite Design	37
4.6.4	Link Budget Design	37
4.7	Electrical Power Subsystem	38
4.7.1	Power Source	39
4.7.2	Energy Storage	41
4.7.3	Power Distribution, Regulation and Control	42
4.7.4	Estimating Total Power Requirement	42
4.7.5	EPS Configuration Analysis	43
4.8	Launcher Selection	47
4.8.1	Electron	48
4.8.2	Soyuz	49
5	Risk Analysis	50
5.1	Structure	50
5.2	Thermal Control	51
5.3	Attitude Determination and Control	51
5.4	Command and Data Handling	52
5.5	Communication	52
5.6	Electric Power Subsystem (EPS)	53

5.7	Launcher	54
6	Conclusions	55
A	Appendix A: Requirements	57
B	Appendix B: ADCS Perturbation Analysis	58
B.1	Gravity Gradient Torque	58
B.2	Solar Radiation Pressure (SRP) Torque	58
B.3	Aerodynamic Drag Torque	58
B.4	Magnetic Torque	58
C	Appendix C: Risk Assessment Criteria	60
D	Appendix D: Launcher loads	62
D.1	Electron	62
D.2	Soyuz	63

List of Figures

3.1	Concurrent Design scheme within the satellite design.	11
3.2	Retro-reflectors array.	12
4.1	Design process description flowchart.	13
4.2	Orbit plane - SS 12AM .	14
4.3	Inclination face needed demonstration.	14
4.4	Scheme of how the inclination of satellite's Zenith face affect period when the satellite can take measures (Configuration with an inclination angle of 15°)	16
4.5	Canisterized Satellite Dispenser.	19
4.6	Tabs included in one of the satellite.	19
4.7	Payload dimension requirements.	20
4.8	ISIS 6-Unit CubeSat primary structure.	20
4.9	Parts manufactured to meet the FOB of Zenit radiometers	21
4.10	Nadir panel	22
4.11	Lateral panels .	22
4.12	Final structure	23
4.13	View of the deploy solution	23
4.14	Subsystem distribution.	24
4.15	Final design CubeSat .	25
4.16	Three-Node distribution front diagram.	28
4.17	Three-Node distribution back diagram.	28
4.18	ADCS trades with other subsystems.	30
4.19	ISIS On Board Computer.	36
4.20	ISIS S-band patch antenna [24]	37
4.21	NanoAvionics CubeSat S-Band Transceiver [25]	37
4.22	NanoAvionics CubeSat S-Band Transceiver [27]	38
4.23	Solar Cell	40
4.24	ISIS Type B Battery [30]	41
4.25	Soyuz propulsion system configuration	49
D.1	Electron Acceleration MPE.	62
D.2	Electron Acoustic MPE.	62
D.3	Electron Random Vibration MPE.	63
D.4	Electron Shock MPE.	63
D.5	Payload acoustic flight loads.	63
D.6	Payload acoustic ground loads.	63
D.7	Payload static and dynamic loads.	64
D.8	Payload shock response.	64
D.9	Payload random loads.	64
D.10	Payload thermal environment.	64

List of Tables

1.1	Teams composition and roles	7
2.1	List of Acronyms	10
2.2	Change Log	10
3.1	Overview of the mission requirements. See Appendix A	11
4.1	Altitude vs Half Angle	14
4.2	Objective areas	17
4.3	Accesses to North Magnetic Pole along 5 days.	17
4.4	Accesses to South Magnetic Pole along 5 days.	17
4.5	Orbit description summary.	17
4.6	Measurement Mode 1.	18
4.7	Measurement Mode 2.	18
4.8	Measurement Mode 3.	18
4.9	R-050 accomplishment using the different measurement modes.	18
4.10	Final satellite properties	25
4.11	Temperature ranges for the on-board components selected for the mission.	26
4.12	Materials and coatings commonly studied for thermal control [12].	27
4.13	Materials and coatings selected for the one-node model.	27
4.14	Temperatures for the one-node analysis for hot and cold cases.	27
4.15	Materials and coatings selected for the three-nodes model.	28
4.16	Temperatures for the tree-node analysis under different solar constant values (Hot case).	29
4.17	Temperatures for the tree-node analysis under eclipse conditions (Cold case).	29
4.18	External Disturbance Torques	30
4.19	Estimated Disturbance Torques	31
4.20	ADCS used in similar missions.	31
4.21	ADCS components listing. (*) Both magnetometer and magnetorquer belong to the same component.	33
4.22	Performance details of the selected sensors [18], [21], [20], [19].	34
4.23	Performance details of the selected actuators. The information is provided for a single actuator [21], [22].	34
4.24	SWaP [18], [20], [19], [22], [21].	34
4.25	Safe-Mode	35
4.26	Science Mode	35
4.27	System Maintenance Mode	35
4.28	Preliminary Link Design	36
4.29	Kiruna Ground Station [23]	36
4.30	Antenna [24]	37
4.31	Transceiver [25]	37
4.32	Link Budget Design	38
4.33	Solar cell specifications.[28]	40
4.34	Battery specifications. [30]	41
4.35	Subsystems power and voltage requirements.	42
4.36	Operating modes for the mission.	43
4.37	Payload Power Consumption	43
4.38	Typical power consumption by subsystem for small satellites (less than 100 W)[26]	44
4.39	POWER BUDGET (I1)	44
4.40	Applied parameters (I1)	45
4.41	Number of Solar Array (I1)	45
4.42	EPS possible configurations	45
4.43	POWER BUDGET (I2)	46
4.44	Applied parameters (I2)	46
4.45	Solar panel power and batteries capacities	47
4.46	Electron's launch sites	48

4.47 Electron's Reliability and Cost	48
4.48 Injection accuracy for 500 km SSO.	49
4.49 Soyuz's launch sites	49
4.50 Soyuz's Reliability and Cost	49
4.51 Injection accuracy for 500 km SSO.	49
5.1 Risks naming convention	50
A.1 Requirements of the MARTINLARA mission.	57
C.1 Severity criteria.	60
C.2 Risk level depending on the likelihood of occurrence	60
C.3 Risk index and magnitude scheme	60
C.4 Proposed actions for individual risks	61

Abstract

This Preliminary Design Review of the MARTINLARA mission has been created following the Product Design Specification document. The purpose of this review is to outline the rationale used to define the preliminary design and its key characteristics. The process began with the investigation of potential design concepts adhering to both the customer and regulatory requirements. The final selection was derived by determining the suitability of each concept as a competitive design for the mission under consideration.

The underlying philosophy driving the selection was balancing achieving the minimum mass and power consumption of the vehicle, whilst understanding the project risks and that the use of proven systems for the components of the vehicle would result in better operational reliability. The overall preliminary configuration has been outlined and, as the process continues into the critical design phase, further detail will be incorporated.

The proposed configuration is based on a 6U CubeSat platform, as that would provide sufficient available volume for the implementation of all the components and systems that must be included to meet the requirements satisfactorily. The satellite will be on a SS-6AM orbit in order to provide the required accesses with the North and South magnetic poles. The power generation will consist of the use of mounted solar panels on 6U face of the satellite, as well as a deployable solar panel array for the 3U sides of the vehicle, as to maximise the power generation at the proposed orbit, a battery will also be included. The ADCS will consist of a redundant active control system that is controlled by the data fed by a variety of sensors. The thermal control of the satellite will be passive, in order to minimise the mass and power consumption of the system and maximise its reliability. The communication subsystem is composed of a transceiver and a patch antenna. Through the proposed design, the MARTINLARA satellite shall meet all the requirements and adhere to all the regulatory requirements imposed by the ECSS documentation.

1. Introduction

This report presents the preliminary analysis and design of the MARTINLARA mission. Firstly, the mission overview will be defined, where the mission requirements and objectives are described. After that, the different subsystems that compound the mission (i.e., Mission Analysis, Structure, Thermal Control, ADCS, Data Handling, Communication and Ground Segment and Electrical Power), as well as the selected launcher, will be defined. Furthermore, a risk analysis of the mission has been included. Finally, the overall conclusions are stated, and a summary table of the adopted solution is provided.

In order to address the mission requirements and constraints in detail, different teams have been in charge of the characterisation of each subsystem previously mentioned. The composition of each team and the subsystem defined by them are the following:

Table 1.1: Teams composition and roles

Members	Subsystem
Javier Vega Mateos Pablo Zapatero Montaña	Mission Analysis
Daniel Del Río Rafael Luque López	Structure & Data handling
Marina Merchán Bravo Daniel Navajas Ortega	Thermal Control
Andrea Bravo Asián Diego Mataix Caballero	ADCS
Laura García Moreno Siro Muela Márquez	Communication
María Alonso Álvarez María Elena Piqueras Carreño	Electric Power

For the definition of the different subsystems, the teams need to interact with one another, either providing input parameters, output parameters, or both. These design parameters have to be continuously updated to reach a compromise solution. Therefore, a proper communication is required. To achieve so, the methodology adopted was that of the Concurrent Design. Usually, this methodology is implemented in a Concurrent Design Facility (CDF). For the development of this preliminary design, a Concurrent Design Application (CDA) has been used instead. Therefore, not only the definition of the vehicle subsystems is carried out, but also a new working environment is tested (CDA).

2. Applicable and reference documents

- [1] California Polytechnic State University. 6U CubeSat Design Specification. 2016.
- [2] 6-Unit CubeSat structure. URL: <https://www.isispace.nl/product/6-unit-cubesat-structure/>.
- [3] SCHATZ BEARINGS, 1900 series. URL: <https://schatzbearing.com/ball-bearing-products/precision-ball-bearings/1900-series/>.
- [4] Dispenser 2002337F-CSD Data-Sheet. URL: <https://www.planetarysystems corp.com/product/canisterized-satellite-dispenser/>.
- [5] 2002367F Payload Spec for 3U 6U 12U. URL: <https://www.planetarysystems corp.com/product/canisterized-satellite-dispenser/>.
- [6] Dispenser 2002337F-CSD Data-Sheet. URL: <https://www.planetarysystems corp.com/product/canisterized-satellite-dispenser/>.
- [7] A. Sanz-Andrés J. Meseguer I. Pérez-Grande. Spacecraft thermal control. Cambridge: Woodhead, 2012.
- [8] SPACECRAFT THERMAL MODELLING AND TESTING. URL: <http://webserver.dmt.upm.es/~isidoro/tc3/Spacecraft%5C%20Thermal%5C%20Modelling%5C%20and%5C%20Testing.pdf>.
- [9] Nanostar Project. URL: <https://nanostar-project.gitlab.io/main/source/preliminary-design/thermal.html>.
- [10] Assal Farrahi and Isabel Grande. “Simplified analysis of the thermal behavior of a spinning satellite flying over Sun-synchronous orbits”. In: Applied Thermal Engineering 125 (July 2017). doi: 10.1016/j.applthermaleng.2017.07.033.
- [11] C. D. Brown. Elements of Spacecraft Design. Reston, Virginia: American Institute of Aeronautics and Astronautics.Inc, 2000.
- [12] Isabel González Rourich. “Desarrollo de un módulo de control térmico para la CDF”. In: (Aug. 2018).
- [13] Malcolm Macdonald and Viorel Badescu. The International Handbook of Space Technology. 2014.
- [14] John O’Sullivan. European Missions to the International Space Station. Reston, Virginia: Springer Praxis Books, 2020.
- [15] Muhammad Nauman Qureshah Abdul Majid Muhammad Naeem Owais. “Aerodynamic Drag Computation of Lower Earth Orbit (LEO)Satellites”. In: (July 2018).
- [16] Le Bonhomme Guillaume. “FORESAIL-2 AOCS trade studies and design”. In: (Aug. 2020).
- [17] GNSS (GPS) accuracy explained. URL: <https://junipersys.com/index.php/support/article/6614>.
- [18] FSS100 Nano fine sensor. URL: <https://satsearch.co/products/tensorotech-fss100-nano-fine-sun-sensor#rfi>.
- [19] ISIS GPS Patch Antenna. URL: <https://www.cubesatshop.com/product/isis-gps-patch-antenna/>.
- [20] Sensonor IMU STIM300. URL: <https://www.sensonor.com/products/inertial-measurement-units/stim300/>.
- [21] ISIS Magnetorquer board. URL: <https://www.isispace.nl/product/isis-magnetorquer-board/>.
- [22] Blue Canyon Technologies - Components. URL: <https://bluecanyontech.com/components>.
- [23] Public.ccsds.org. URL: <https://public.ccsds.org/Pubs/411x0g3s.pdf>.
- [24] ISIS “CubeSat S-band patch antenna” ISIS.SPPA.DS.00001 datasheet, version 1.4.
- [25] NanoAvionics. Cubesat S-Band Transceiver — Nanoavionics. URL: <https://public.ccsds.org/Pubs/411x0g3s.pdf>.
- [26] W. Larson and J. Wertz. Space Mission Analysis And Design. Dordrecht: Kluwer Academic Publishers, 2005.
- [27] NanoAvionics. Cubesat S-Band Transceiver — Nanoavionics. URL: <https://en.wikipedia.org/wiki/Eb/N0>.
- [28] AzurSpace. GaAs Solar Cell — AzureSpace. URL: https://www.azurspace.com/images/006050-01-00_DB_3G30C-Advanced.pdf.
- [29] ISISPACE. Solar Panels — ISISPACE. URL: <https://www.isispace.nl/product/isis-cubesat-solar-panels/>.

- [30] ISISPACE. EPS — ISISPACE. URL: https://www.isispace.nl/wp-content/uploads/2019/04/ISIS-iEPS2_0-DS-00001-iEPS_Datasheet-1_0.pdf.
- [31] ECCS-M-ST-80C. Risk Management.

Acronyms

Table 2.1: List of Acronyms

Acronym	Definition
ADCS	Attitude Determination and Control System
BER	Bit Error
CAD	Computer-Aided Design
CDA	Concurrent Design Application
CDF	Concurrent Design Facility
CMG	Contron Moment Gyroscopes
CoM	The Center of Mass
COST	Commercial Off-The-Shelf Components
CSD	Canisterized Satellite Dispenser
DoD	Depth of Discharge
EPS	Electric Power Subsystem
ESA	European Space Agency
FoS	Factor of Safety
FOV	Field Of View
GMSK	Gaussian Minimum Shift Keying
GNSS	Global Navigation Satellite System
GPS	Global Positioning System
IMU	Inertial Measurement Unit
iOBC	ISIS On Board Computer
ISIS	Innovative Solutions In Space
LEO	Low-Earth Orbit
MLI	Multi Layer Insulation
MPPT	Maximum Power Point Tracker
NMP	North Magnetic Pole
PCU	Power Control Unit
PDU	Power Distribution Unit
PPT	Plasma Pulse Thruster
RGT	Repeating Ground Track
SLR	Satellite Laser Ranging
SP	Solar Panels
SRP	Solar Radiation Pressure
SSO	Sun-Synchronous Orbit
SWaP	System Weights and Power
U	Cubesat Unit
UCM3	Universidad Carlos III

Change Log

Table 2.2: Change Log

Edition/Revision	Date	Description of the change
V0.0	20/12/2020	Initial version of the document
V0.1	23/12/2020	Added the various subsystems
V0.2	30/12/2020	Changed the format from article to report
V1.0	09/01/2021	Added the introduction, abstract and conclusions
V1.1	10/01/2021	Final changes

3. Mission overview, requirements flow-down

The proposed mission is part of the MARTINLARA project, whose objective is to design an in-orbit technological demonstration mission for the development of various technologies with the aim of validating them for space use. Therefore, the project involves the development of a nanosatellite platform for the in-orbit validation of such technologies, whose design must conform to six top-level objectives. These include the demonstration of technologies for radio-astronomy, Earth observation and plasma micropropulsion, as well as the observation of the Earth and the Microwave Cosmic Background using the on-board experimental technologies.

The current design for the MARTINLARA project, outlined in this PDR, has been produced to satisfy the customer and the relevant regulatory bodies. Each part of the design either meets the requirement functionally, i.e. in its design the system conforms to the requirement or through constraint, where the design parameters are defined by the requirement. The design components of this review have been separated into the various subsystems: Communication, Data Handling, ADCS, EPS, Mission Analysis, Thermal Control and Structures. Each sub-section details the design elements associated with that section where consideration at this stage was deemed important. The various conceptual design options explored for said elements are then outlined, followed by the constraints/rationale used to inform our choice. Table 3.1 shows the requirements and the goals that have been met.

Table 3.1: Overview of the mission requirements. See Appendix A.

Requirement	R-010	R-020	R-030	R-040	R-050	R-060	R-070	R-080	R-090	R-100
Met	<i>Minimum</i>	YES								
	<i>Goal</i>	N/A	N/A	N/A	N/A	YES	N/A	YES	N/A	N/A
Requirement	R-110	R-120	R-130	R-140	R-150	R-160	R-170	R-180	R-190	R-200
Met	<i>Minimum</i>	YES								
	<i>Goal</i>	N/A	N/A	N/A	N/A	YES	YES	N/A	N/A	N/A

Following the imposed requirements of the mission, the satellite design provides a compromise solution between all the aforementioned subsystems. To achieve that, the Concurrent Design approach has been implemented, enabling the communication between the different subsystems to iteratively define the final configuration. Reaching the proposed design required different inputs and outputs from each subsystem, as Figure 3.1 highlights. In favour of concision, this inputs and outputs will be identified within each subsystem section.

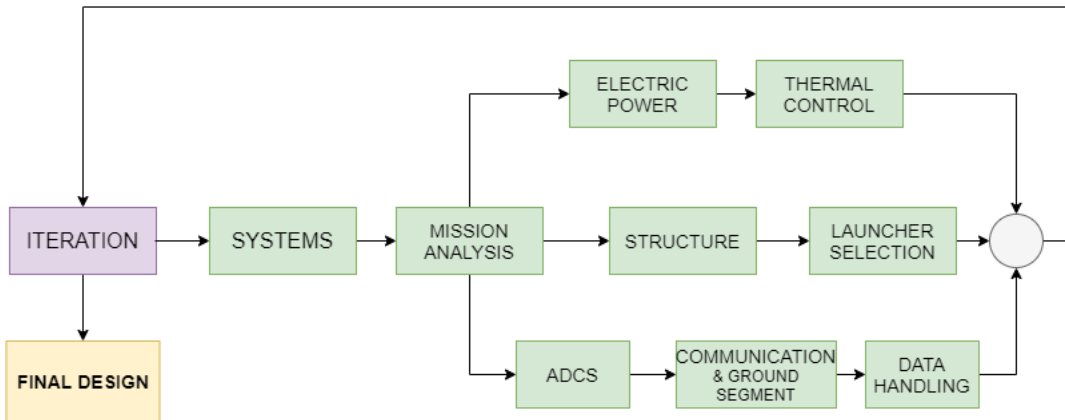


Figure 3.1: Concurrent Design scheme within the satellite design.

The mission payload are presented in the following points:

- **Photonic payload**

The main payload consists of three pairs of photonic radiometers, since each pair is composed of one radiometer that points to Zenith and another terrestrial one, which points to Nadir. This payload entails a new technology for signal detection of millimetric waves at ambient temperature, so cryogenic temperatures are not necessary

for this purpose.

Moreover, the study is made within three wavebands (180 GHz, 200 GHz and 250 GHz), that is why three pairs of radiometers are needed. It must be considered that each radiometer is connected to its antenna, as they work in pairs in order to obtain crossed measurements.

- **Micropropulsion system**

An electric micropropulsion system is included in order to verify its correct operation in space. It starts to operate at the last phase of the mission, so that it does not interfere with the main payload. It must be ensured that one face pointing to the outside which shall be obstacle free exists.

- **Retro-reflectors array**

An array composed of four retro-reflectors, which is shown in Figure 3.2, is attached in the satellite Nadir face. This payload provides the distance between the satellite and SLR (Satellite Laser Ranging) stations, so it allows for determining orbit parameters as well.

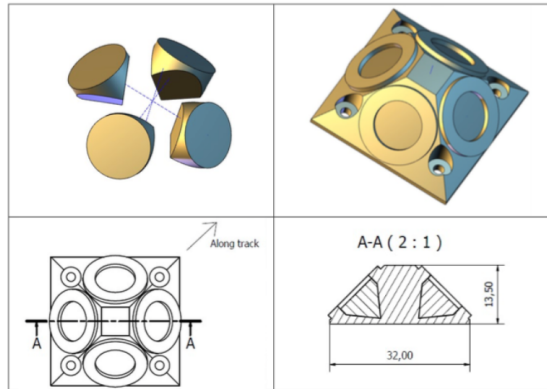


Figure 3.2: Retro-reflectors array.

4. Subsystem analysis and design

4.1 Mission Analysis

4.1.1 Introduction

The Mission Analysis deals with the outer space environment and it is focused on searching a solution for the most suitable orbit that accomplishes the specified requirements for the payload provided from the customer. The orbit design shall be the first step within the whole process of designing a space mission. Our decisions will be based on the following set of requirements: **R-030, R-040, R-050, R-060, R-070, R-090, R-100, R-130, R-140** and **R-150**.

The definition process will consist of four phases:

- Orbit parameters determination to fulfil the minimum goals presented in the requirement list.
- Detailed definition for aiming to reach the top goals.
- Share parameters proposal with other subsystems.
- Iteration process with other subsystems to reach the best overall solution.

The iteration cycle can be observed in the figure (4.1) below:

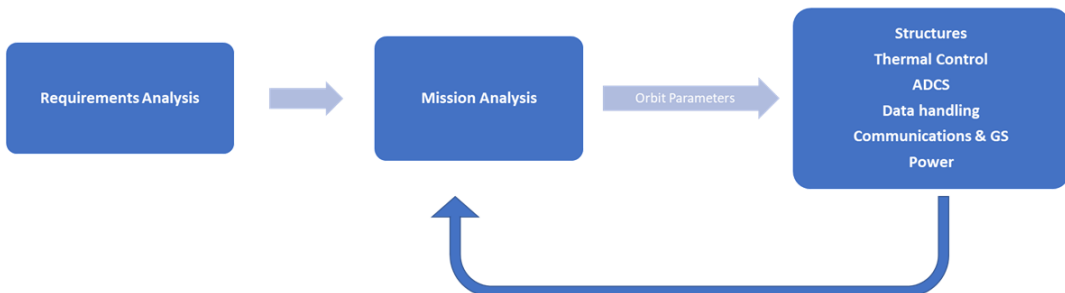


Figure 4.1: Design process description flowchart.

As it can be seen the Mission Analysis subsystem has, at first, no inputs from other subsystems and provides the base for the rest of the satellite definition.

4.1.2 Orbit analysis

In order to give an initial orbit proposal, all the requirements involved with the orbit definition are going to be studied.

- **Nadir Antennas:**

Considering Nadir antennas will be always pointing to subsatellite point on Earth, along its normal, with a maximum deviation of $\pm 5^\circ$, they will be always free of the Sun and other spacecraft obstacles, so requirement **R-070** is fulfilled.

Requirement **R-140** will be directly related to orbit altitude and to the field of view of the instrument. Therefore, to accomplish this requirement it has been considered that the instrument is always pointing along its normal so that the track over the Earth surface would be always a circle. In order to determine the maximum field of view at each altitude, a quick analysis has been developed by splitting the range of altitudes between [400, 550] km into 30 km intervals. The table bellow shows the results.

Table 4.1: Altitude vs Half Angle

Altitude (km)	Half Angle ($^{\circ}$)
400	3.576
430	3.327
460	3.111
490	2.92
520	2.7525
550	2.603

- **Zenith Antennas:**

Valid measurements of the radiometers must be taken free of the Sun, Earth and other spacecraft obstacles. Firstly, the interaction between the antennas and the Sun is studied. The first thought to spring to mind if we are determining an orbit basing on the Sun behavior is a Sun Synchronous orbits. Through further analysis, and in order to keep the zenith antenna's FOV away from the Sun direct incidence, it seems reasonable to fix the satellite to get the sun rays always in the lateral direction. Otherwise, there will be always a period in every orbit cycle in which the Zenith antennas are receiving direct light from the Sun, as it can be seen in the following picture:

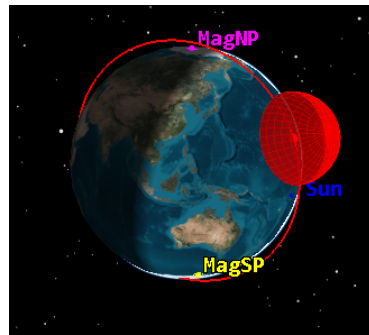


Figure 4.2: Orbit plane - SS 12AM

All things considered, the first orbit trajectory proposal is a Dawn-Dusk Sun Synchronous orbit, which allows to fulfil the requirement **R-040**.

To provide a brief analysis of the Sun intrusion into Zenith antennas FOV, the worst-case scenario, when the Earth is passing through the Perigee/Apogee, will be studied:

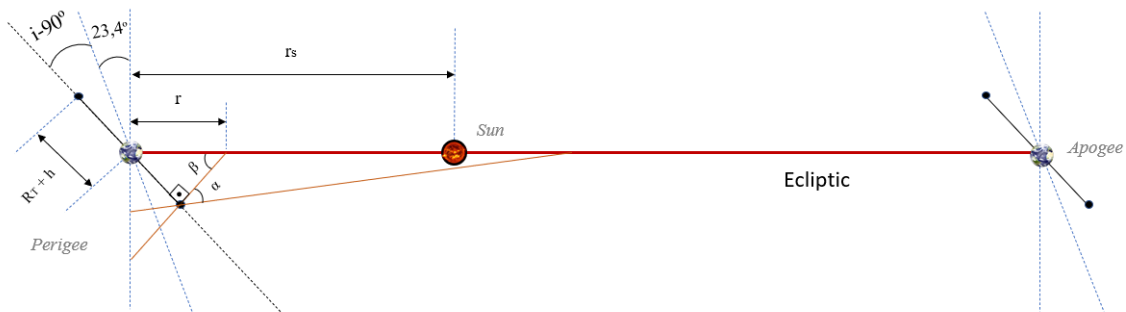


Figure 4.3: Inclination face needed demonstration.

Sun avoidance of zenith antennas must meet the next condition:

$$r > r_s \quad (4.1)$$

Having an Earth-Sun distance at perihelium of:

$$r_s = 147.500.000 km$$

The r for generic values of the inclination i was calculated:

$$r = \frac{R_T + h}{\sin(\beta)} = \frac{R_T + h}{\sin(23.4^\circ + (i - 90^\circ))} \quad (4.2)$$

Introducing a common value of i for Sun-Synchronous orbits ($i=97^\circ$) and a reasonable orbit altitude within the limits imposed by requirement **R-030** ($h=500km$) it returns:

$$r = 13591.97 km \ll r_s \quad (4.3)$$

Then, it becomes necessary to include an angled face for zenith antennas (α in the picture) to avoid Sun interference.

At this point, it is important to fix a maximum face angle to keep the Earth out of the zenith antennas, attending to **R-100**. The maximum angle will appear when the zenith FOV becomes tangent to the Earth surface. So that:

$$\sin(\alpha_{max} - 90^\circ) = \frac{R_T}{R_T + h} \quad (4.4)$$

Inserting a feasible value ($h=500km$) considering the maximum altitude required, the maximum face angle for which the top face can be inclined to meet requirement **R-100** is calculated:

$$\alpha_{max} = 21.98^\circ$$

It has been left clear that in order to star fixing the design orbit parameters, a design value for the orbit altitude is needed.

4.1.3 Mission duration and access study

To develop this analysis the SKT and GMAT software packages will be used. The former in order to study the accesses and the eclipse periods and the latter to get some information about the satellite's orbit decay employing GMAT's atmospheric drag model. In the figure 4.4 it can be seen how the zenith FOV interacts with the Sun within a period of a year. The picture shows the variation on the sunlight angle with respect to the equator plane during a year, the maximum value corresponds to the ecliptic plane angle. The relation between the face inclination angle and the period for which its free from direct sunlingth is immediate. The green line represents the moment when the sun rays and the orbit plane are perpendicular, which is the unique instant when the requirement **R-100** could be met without having to lean the satellite's zenith face. It easy to see how by tilting this face an angle of α degrees, a period of α degrees free of sun light incidence on the zenith face is achieved .

As it can be seen, the altitude and the face angle will be decisive for determining the period of time when the measures can be taken. Thus, the greater face angle we take the longer time we will be able to take measurements. Considering the altitude of the orbit, it was firstly implemented an altitude of:

$$h = 410 km \quad (4.5)$$

It was set to force the orbit to be repeating ground track with a ground track repeated each two days. This would definitely ease the calculations for measurements accesses in this phase of design.

However, at this altitude the satellite would loose a significant altitude due to the aerodynamic drag during the 3 months of operations defined in the **R-070** as goal:

$$\Delta h_{loss}(h = 410 km) = -75.53 km$$

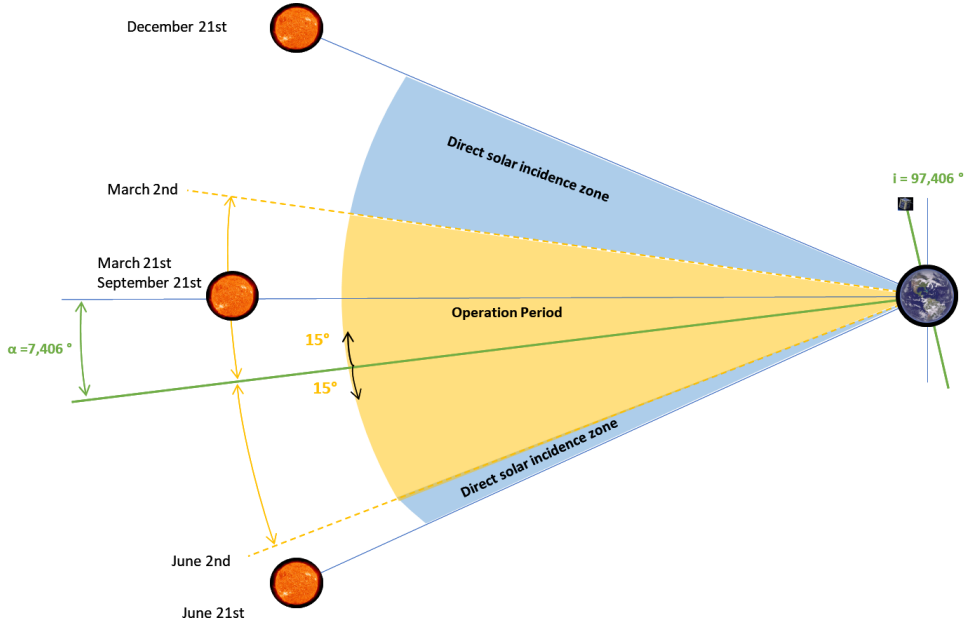


Figure 4.4: Scheme of how the inclination of satellite's Zenith face affect period when the satellite can take measures (Configuration with an inclination angle of 15°)

That would affect, not only to our first approximation, a repeating ground track orbit, but more importantly, to our satellite's performance and its capacity to have a decent lifetime because of the lack of any propulsion system to make orbit corrections. Therefore, in order to minimize this inconvenient, we have decided to raise up the orbit altitude up to 500 km where, due to the low particle's density, the drag becomes less relevant. This consideration places the satellite between the limits dictated by **R-030**. Within this configuration, the altitude decay for 3 months of operations is:

$$\Delta h_{loss}(h = 500\text{km}) = -14\text{km}$$

That involves a relative error with respect to the nominal orbit of:

$$\epsilon = \frac{h_{inicial} - h_{final}}{h_{inicial}} = 2.8\% \quad (4.6)$$

That is about the injection accuracy's order of magnitude of the majority of the launchers. Hence it is an assumable deviation from nominal trajectory.

Once the altitude is selected, we proceed to do the same with the face inclination angle. To reach the minimum requirement of measuring for 1 month, for the selected altitude, it is needed:

$$\alpha = 4.83^\circ$$

However, aiming to the target of obtaining 3 months of valid measurements and without having any trouble with the other subsystems, the selected face angle shall be:

$$\alpha = 15^\circ$$

Now we have enough information from the orbit to make an access study.

Building up a model, given by all the parameters that have been mentioned, STK returns us a period of operation of 3 months, from the 2nd of March to the 2nd of June.

To finally fix the mission duration, the position of the objective areas and of the ground station are defined.

Table 4.2: Objective areas

Objective	Latitude	Longitude
North Magnetic Pole	$\phi = 86.448^\circ N$	$\lambda = 175.3458^\circ E$
South Magnetic Pole	$\phi = 64.28^\circ S$	$\lambda = 136.59^\circ E$
Kiruna Ground Station	$\phi = 67.857^\circ N$	$\lambda = 20.964^\circ E$

After implementing the target areas, the ground stations and the orbit design parameters, the accesses study can be done. A period of 5 days since it is the period of track repetition has been studied, and as seen before, the altitude decay will almost not affect the satellite's performance and mission analysis calculations.

Table 4.4: Accesses to South Magnetic Pole along 5 days.

Access #	Start Time (UTC)	Stop Time (UTC)	Duration (sec)
1	2 Mar 2021 10:48:40.868	2 Mar 2021 10:49:55.907	75.039
2	2 Mar 2021 12:22:55.833	2 Mar 2021 12:24:23.606	87.773
3	2 Mar 2021 13:57:25.524	2 Mar 2021 13:58:37.104	71.580
4	3 Mar 2021 10:29:51.850	3 Mar 2021 10:30:59.810	67.960
5	3 Mar 2021 12:04:03.774	3 Mar 2021 12:05:31.319	87.545
6	3 Mar 2021 13:38:30.054	3 Mar 2021 13:39:47.585	77.531
7	4 Mar 2021 10:11:03.966	4 Mar 2021 10:12:02.220	58.254
8	4 Mar 2021 11:45:12.260	4 Mar 2021 11:46:38.505	86.245
9	4 Mar 2021 13:19:35.415	4 Mar 2021 13:20:57.475	82.059
10	4 Mar 2021 14:54:23.475	4 Mar 2021 14:54:56.243	32.768
11	5 Mar 2021 09:52:18.003	5 Mar 2021 09:53:02.141	44.138
12	5 Mar 2021 11:26:21.269	5 Mar 2021 11:27:45.088	83.819
13	5 Mar 2021 13:00:41.642	5 Mar 2021 13:02:06.659	85.017
14	5 Mar 2021 14:35:21.056	5 Mar 2021 14:36:12.553	51.497
15	6 Mar 2021 09:33:38.972	6 Mar 2021 09:33:55.051	16.079
16	6 Mar 2021 11:07:30.787	6 Mar 2021 11:08:50.857	80.070
17	6 Mar 2021 12:41:48.452	6 Mar 2021 12:43:15.377	86.925
18	6 Mar 2021 14:16:22.369	6 Mar 2021 14:17:25.546	63.176

Table 4.3: Accesses to North Magnetic Pole along 5 days.

Access #	Start Time (UTC)	Stop Time (UTC)	Duration (sec)
1	2 Mar 2021 08:19:07.622	2 Mar 2021 08:21:01.866	114.244
2	2 Mar 2021 21:11:28.218	2 Mar 2021 21:11:41.853	13.635
3	3 Mar 2021 08:00:03.591	3 Mar 2021 08:02:28.403	144.813
4	3 Mar 2021 22:25:48.824	3 Mar 2021 22:27:39.075	110.251
5	4 Mar 2021 07:41:16.932	4 Mar 2021 07:43:42.136	145.204
6	4 Mar 2021 22:06:48.642	4 Mar 2021 22:09:11.310	142.668
7	5 Mar 2021 07:22:45.906	5 Mar 2021 07:24:44.408	118.501
8	5 Mar 2021 21:48:00.500	5 Mar 2021 21:50:27.226	146.726
9	6 Mar 2021 07:04:50.908	6 Mar 2021 07:05:14.823	23.915
10	6 Mar 2021 21:29:24.306	6 Mar 2021 21:31:26.716	122.410

Special care has been taken with respect to the requirements **R-060** and **R-130**. The mission length is finally estimated, adding the launch campaign and the launch itself:

$$t_{mission} = 90 + 10\text{days} \quad (4.7)$$

Therefore, the goal for **R-070** would be accomplished.

4.1.4 Results

Table 4.5: Orbit description summary.

Parameter	Description
$i = 97.406^\circ$	Fixes the orbit as SS-6AM of LTAN
$h = 500\text{km}$	Fixes the orbit as RGT repetition period: 5 days
$\text{ecc} = 0$	Circular orbit
$\text{RAAN} = 180^\circ$	
$\text{AOP} = 0^\circ$	
$T = 5576.81 \text{ seg}$	Period around 1h30
$\alpha = 15^\circ$	Allows 3 months free of Sun
$\alpha_{max} = 21.98^\circ$	Upper limit
$\eta = 2.8624^\circ$	Nadir HA for measurements
$t_{max,eclipse} = 0 \text{ seg}$	Total absence of eclipses during operation
$t_{mission} = 100 \text{ days}$	Starting from launch.
$L_{date} 28^{\text{th}} \text{ February}$	Ideal launch date.
$V_{orb} = 7662.62 \frac{\text{m}}{\text{s}}$	Launcher interface
$Irr = [1321.1, 1412.9] \frac{\text{W}}{\text{m}^2}$	Power interface

4.1.5 Measurements Modes

Attending to the requirement **R-050**, three different measurements modes have been proposed: **MM-1**, **MM-2** and **MM-3**. Others modes could be studied, and for this purpose the accesses tables to the North and South Magnetic Poles have been provided. The tables bellow show the 3 modes defined for a period of five days since the first day of operation proposed. As we have selected a RGT orbit this study is valid for the whole period of operation proposed.

Table 4.6: Measurement Mode 1.

MM-1						
Paso por Kiruna	Measure 1 (North Magnetic Pole)	Measure 3 & 4 (North Magnetic Pole)	Paso por Kiruna	Measure 4 (North Magnetic Pole)		
02-03-2021 02:49:14	02-03-2021 08:19:07	02-03-2021 09:52:03	02-03-2021 10:48:40	02-03-2021 15:27:28	02-03-2021 17:13:02	02-03-2021 21:11:28
03-03-2021 04:04:51	03-03-2021 08:00:03	03-03-2021 09:32:59	03-03-2021 10:29:51	03-03-2021 15:08:39	03-03-2021 18:28:09	03-03-2021 22:25:48
04-03-2021 03:45:26	04-03-2021 07:41:16	04-03-2021 09:14:12	04-03-2021 10:11:03	04-03-2021 16:22:47	04-03-2021 18:09:05	04-03-2021 22:06:48
05-03-2021 03:26:29	05-03-2021 07:22:45	05-03-2021 08:55:41	05-03-2021 09:52:18	05-03-2021 16:04:02	05-03-2021 17:50:13	05-03-2021 21:48:00
06-03-2021 03:07:45	06-03-2021 07:04:50	06-03-2021 08:37:46	06-03-2021 09:33:38	06-03-2021 14:12:26	06-03-2021 17:31:31	06-03-2021 21:29:24
						06-03-2021 23:02:20

Table 4.7: Measurement Mode 2.

MM-2					
Connection with Kiruna	Measure 1 (North Magnetic Pole)	GS connection	Measure 2 (South Magnetic Pole)		
02-03-2021 02:49:14	02-03-2021 10:48:40	02-03-2021 12:21:36	02-03-2021 17:13:02	02-03-2021 21:11:28	02-03-2021 22:44:24
03-03-2021 04:04:51	03-03-2021 10:29:51	03-03-2021 12:02:47	03-03-2021 18:28:09	03-03-2021 22:25:48	03-03-2021 23:58:44
04-03-2021 03:45:26	04-03-2021 10:11:03	04-03-2021 11:43:59	04-03-2021 18:09:05	04-03-2021 22:06:48	04-03-2021 23:39:44
05-03-2021 03:26:29	05-03-2021 09:52:18	05-03-2021 11:25:14	05-03-2021 17:50:13	05-03-2021 21:48:00	05-03-2021 23:20:56
06-03-2021 03:07:45	06-03-2021 09:33:38	06-03-2021 11:06:34	06-03-2021 17:31:31	06-03-2021 21:29:24	06-03-2021 23:02:20

Table 4.8: Measurement Mode 3.

MM-3				
Connection with Kiruna	Measure 1		Measure 2	Connection with Kiruna
02-03-2021 02:49:14	02-03-2021 10:48:40 (NMP)	02-03-2021 12:21:36	02-03-2021 12:21:36 (NMP)	02-03-2021 13:54:32
03-03-2021 04:04:51	03-03-2021 08:00:03	03-03-2021 09:32:59	03-03-2021 22:25:48	03-03-2021 23:58:44
04-03-2021 03:45:26	04-03-2021 10:11:03 (NMP)	04-03-2021 11:43:59	04-03-2021 11:43:59 (NMP)	04-03-2021 13:16:55
05-03-2021 03:26:29	05-03-2021 07:22:45	05-03-2021 08:55:41	05-03-2021 21:48:00	05-03-2021 23:20:56
06-03-2021 03:07:45	06-03-2021 09:33:38 (NMP)	06-03-2021 11:06:34	06-03-2021 11:06:34 (NMP)	06-03-2021 12:39:30
				06-03-2021 17:31:31

After an iterative process with the Electrical Power Subsystem two different ways of accomplish the requirement **R-050** have been defined. On the one hand, to meet the requirement for taking measurements using one pair of radiometer, on the other hand, to accomplish the goal specified in this requirement, taking measures using two pairs of radiometers at once.

Table 4.9: R-050 accomplishment using the different measurement modes.

Requirement R-050		MM-1	MM-2	MM-3
Met	Minimum	YES	YES	YES
	Goal	NO	YES	NO

4.2 Structure subsystem

In this section, all aspects regarding the structure and the general satellite configuration will be discussed. This includes the selection of the off-the-shelf components employed, and the description of the required manufactured parts, as well as the positioning of all satellite elements in the final assembly.

4.2.1 Satellite Dispenser

This satellite will be transported together with other payloads as a secondary or tertiary payload of a shared launch. For the deployment of the satellite and its interface with the launcher vehicle, a satellite dispenser will be necessary.

In this section, a satellite dispenser system will be selected. The requirements imposed by the satellite dispenser and the structural modifications needed by the satellite/dispenser interface will also be explained.

The dispenser selected is the Canisterized Satellite Dispenser, Figure 4.5, manufactured by Planetary Systems Corporation. The Canisterized Satellite Dispenser (CSD) is a reliable, testable, and cost-effective deployment mechanism for small secondary or tertiary payloads. It fully encapsulates the payload during launch and thus provides mission assurance for both the primary payload and launch vehicle.

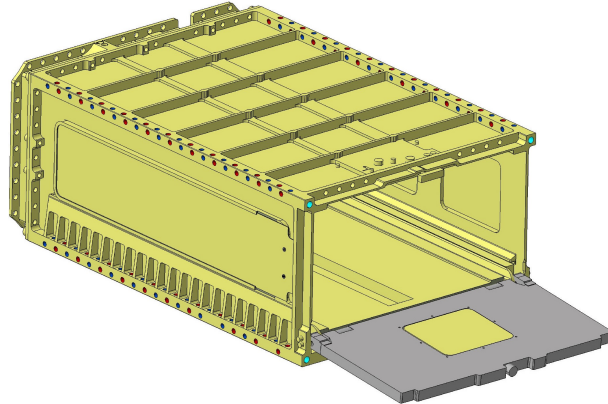


Figure 4.5: Canisterized Satellite Dispenser.

The most distinctive feature of this dispenser is the interface with the satellite. The payloads incorporate two tabs running the length of the ejection axis. The CSD will grip these tabs, providing a secure, modelable, preloaded junction. This is essential to accurately predict loads on critical components and instrumentation and prevent jiggling.

Both the tab and the material chosen, Aluminium 7075-T7351, for this project have been extracted from the Dispenser Data-Sheet, [5]. The CAD model can be seen in Figure 4.6



Figure 4.6: Tabs included in one of the satellite.

This simple interface with the dispenser will allow for more freedom in the structural design. Concretely, it allows for the inclination of the Zenit face described in the following sections, allowing all faces of the satellite to change as long as the satellite follows the specification provided by the CSD manufacturer.

A payload can be built to this specification without knowledge of the specific dispenser within it will fly. Similarly, dispenser manufacturers will be ensured of compatibility with payloads that conform to this specification.

The most important requirements can be summarized in 4 points:

- Dimensional and material requirements are provided for the tabs.
- Maximum dimensions and tolerances ($366 \times 239 \times 116$ mm 3 figure 4.7) shall be maintained under all temperatures.
- The structure comprising the $-Z$ face (face that contacts CSD ejection plate) may be a uniform surface or consist of discrete contact points. The discrete contact points shall be located such that they envelope the payload's C.M. and any deployment switches.
- The Center of Mass (CoM) shall be located within a certain range referred to the geometric center of the CubeSat. [1].

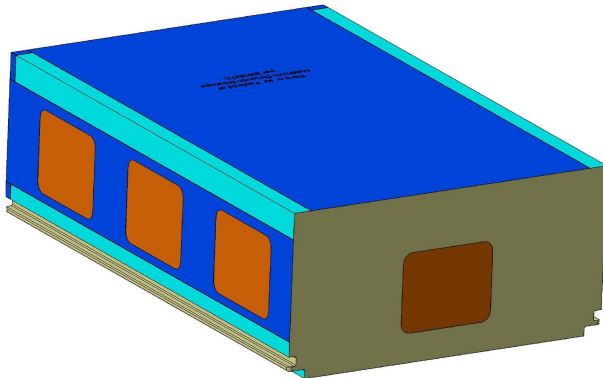


Figure 4.7: Payload dimension requirements.

The full requirements are available in the specifications document provided by Planetary Systems Corporation [5].

The figure 4.7 shows the required payload dimensions, where the orange represents accessible areas, and any geometry contained within this envelope will be valid.

The last important design feature related with the pod is the necessity of a connector between the satellite and the CSD, this connector is sold by the same company, and it's specifications can be found in their website [6].

4.2.2 Primary structure

For the design of a satellite structure it is essential to ensure that it will withstand launch loads. However, as a CubeSat uses deployers to fix them to the launcher, it is the deployers which guarantee structural integrity under launch loads.

The fact that CubeSat structures do not have to withstand high loads makes it easy to find standard commercial structures on the market following with the Commercial Off-The-Shelf Components (COST) philosophy.

In this mission, we started with a 3 payloads that occupied 1U each one. This has made that the standardized CubeSat size chosen has been 6U. The selected structure is the *ISIS 6-Unit CubeSat structure*, [2]. It has flight heritage since 2016 and includes the side panels along with the necessary hardware for assembly. In this way, the **R-010** and **R-020** requirements are met.

The primary structure CAD can be seen in Figure 4.8 with a total weight of 789 grams. Side panels weight have not been added as modifications will be made to achieve full payload functionality.

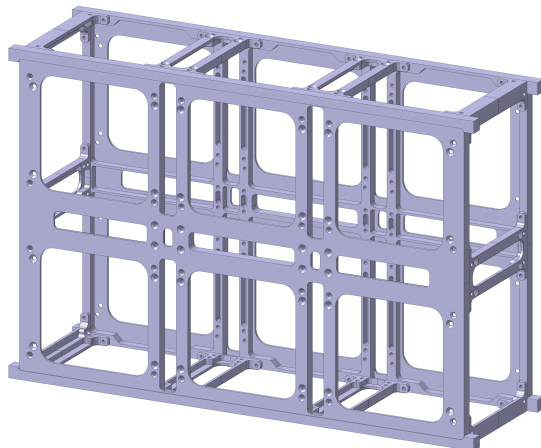


Figure 4.8: ISIS 6-Unit CubeSat primary structure

4.2.3 Manufactured components

Payload requirements make a brand new structure not entirely mission-appropriate. Therefore, the manufacture of certain parts is mandatory.

However, the solution that has been sought is based on easily machinable parts and aluminum sheets for laser cutting, so overrun is minimum.

This subsection will be divided into three groups depending on the area where the pieces are located.

- **Zenith**

The requirement **R-100** has made necessary to further modify the COST structure related to the Zenith's radiometers. The cause is that these radiometers shall have the FOV free of Sun, Earth and spacecraft obstacles during operation. In addition, the material used is aluminum 7075-T7351, the same one chosen for the tabs.

Due to the chosen orbit it was necessary to tilt the surface of the radiometers a minimum of 9 degrees. However, to avoid possible problems due to unexpected disturbances, this inclination has been increased to 15°.

To achieve this inclination without modifying the primary structure, three aluminium pieces (extensions) have been designed together with a folded sheet that manages to hide the radiometers from the sun.

The extensions are screwed to the spacers of the main structure in their standard holes. Once the extensions are attached, the plate is screwed onto them to close the CubeSat.

The manufactured parts can be seen in Figure 4.9 with a total weight of 289 grams.

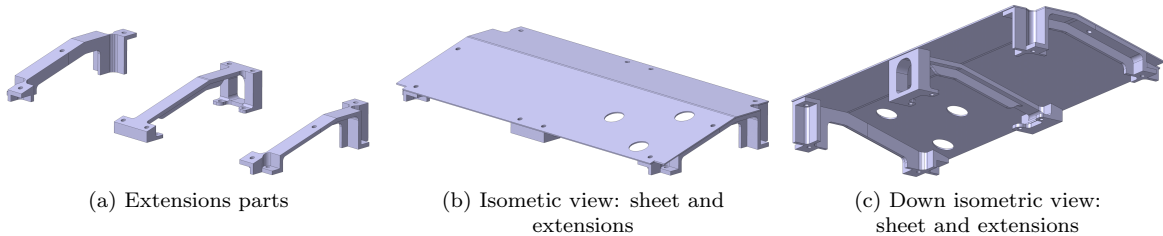


Figure 4.9: Parts manufactured to meet the FOB of Zenit radiometers

- **Nadir**

Instruments that target Nadir have less restrictive FOV requirements (**R-090**). This CubeSat face houses Nadir's trio of radiometers, the retroreflectors array and the communication antenna. Due to this agglomeration of instruments the Nadir panel needs more rigidity than the Zenith's.

For the manufacture, an aluminum 7075-T7351 block has been machined to make the connection holes and a box where the retro-reflectors are housed. The radiometers holes have a chamfer of 65° that allows them to measure without interfering with their FOV.

Due to the increase in CubeSat's enveloping length caused by Zenith extension, the retroreflectors have to be sunk into the panel ought to comply with the CSD maximum envelope (366 mm).

To avoid interference between the antenna and the retroreflectors, they have been distanced and a chamfer has been made to the retroreflector box.

The Nadir panel can be seen in Figure 4.10 with a total weight of 186 grams.

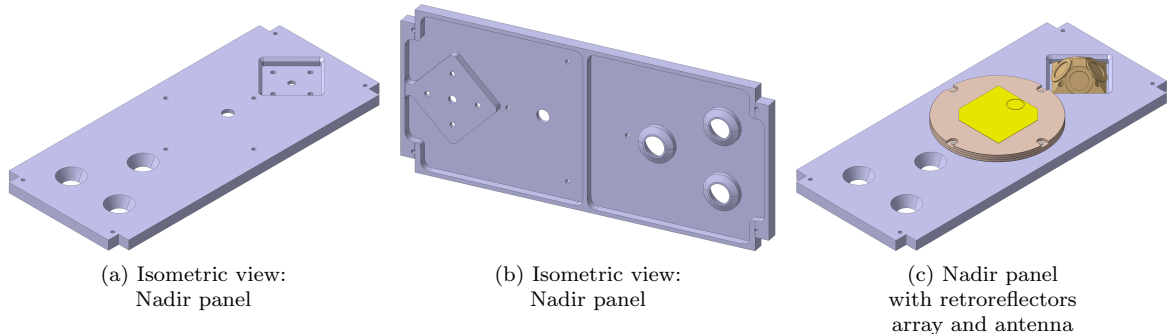


Figure 4.10: Nadir panel

- **Side panels**

The side panels are simply 0.8 mm laser cutted aluminum sheets that close the CubeSat.

The plates cover the entire outer surface, so the 6U faces are different since the one perpendicular to the sun is slightly longer than the one in shadow.

On the other hand, the 3U side panels are also different, since the one whose normal is coincident with the velocity vector has a hole for the nozzle of the last payload, the microengine (requirement **R-190**).

The four lateral panels can be seen in Figure 4.11 with a total weight of 436 grams.

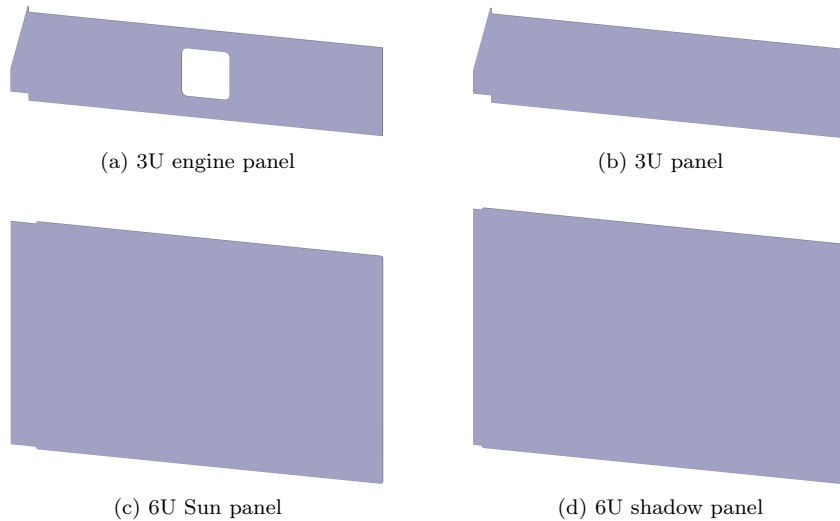


Figure 4.11: Lateral panels

Finally, once the dispenser rails are added, the structure has a total weight of 1550 grams and the CAD model can be seen in Figure 4.12

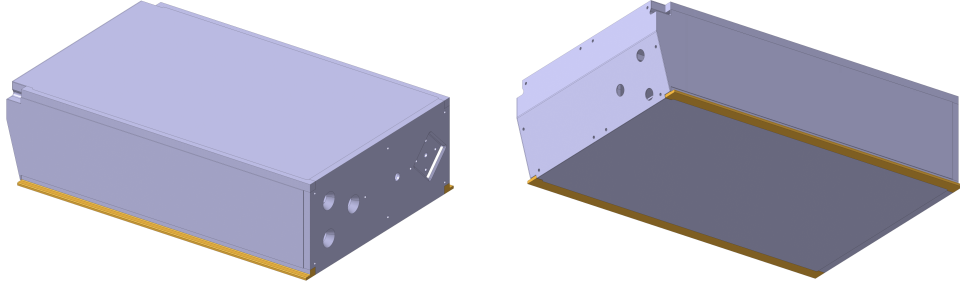


Figure 4.12: Final structure

4.2.4 Deployable solar panel

As it will be discussed in the power section, a solar panel that fills the 6U face does not get enough power to feed both payloads and subsystems. Therefore, it has been concluded that deploy two panels of the 3U sides is necessary.

In this section we are going to focus on the integration of these deployable panels in the CubeSat.

- A simple solution based on two bearings has been found to keep the panels folded during launch. These bearings are located at the opposite end of the hinges and are in contact with the dispenser. Once the dispenser ejects the CubeSat, the panels will roll on the surface of the dispenser and once they are fully removed they will open. These bearings can be founded in [3].
- The panel opening mechanism consists of a torsionally loaded hinge. Once the CubeSat is ejected from the deployer, the hinges will rotate the deployable panels to their final position.

This solution can be seen in Figure 4.13

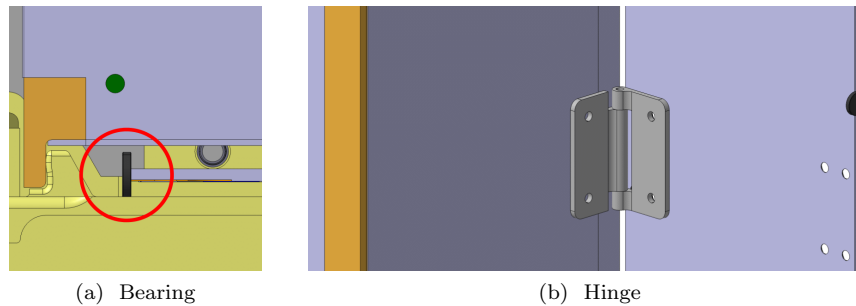


Figure 4.13: View of the deploy solution

The weight added to the CubeSat through the panels is 135 grams for the combination of the 3U panel, bearings and hinges (270 grams for both panels) and 200 grams for the 6U panel. All panels add 335 grams to the weight of the CubeSat.

4.2.5 Subsystem distribution

Once the structural design is completed, we will assign a space in the satellite to all the components and subsystems, defining the configuration of the satellite. The most important point to take into consideration for this distribution is the positioning of the center of mass. The center of mass shall be located near the geometrical center of the primary structure, within the limits provided by the cubesat standard an the pod's manufacturer [5] and [1]. Taking this into consideration, all components are represented in a simplified way in CATIA, introducing the adequate masses and volumes. Several configurations are analyzed, until the following one is chosen:

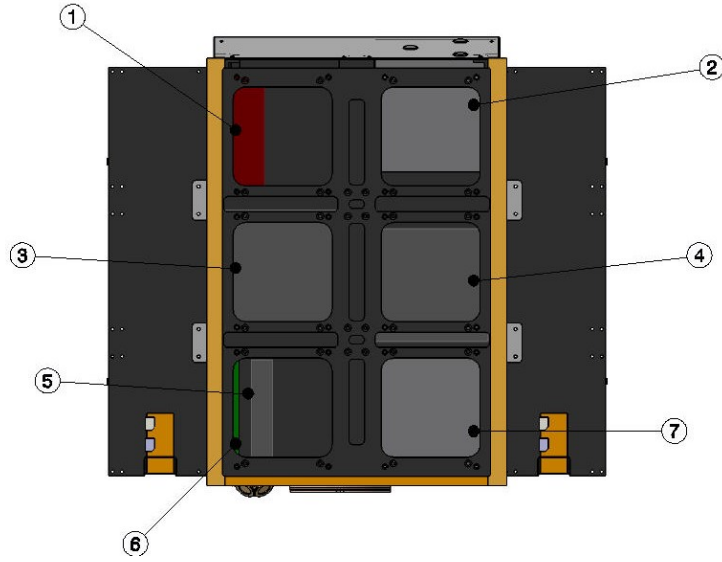


Figure 4.14: Subsystem distribution.

Where the different components are: (1) Battery, (2) Zenith photonic payload, (3) Micropulsion system, (4) ADCS, (5) Transciever, (6) On-board computer, (7) Nadir photonic payload.

The position and orientation of the elements (1), (5) and (6) within their units is designed for keeping the CoM near the geometrical center of the primary structure. On the other hand, the positioning of the elements (3) and (4), some of the more massive elements, near the center also intends to center the CoM and reduce the inertia. Lastly, this configuration provides the micropulsion system with an opening aligned to the center of mass, increasing the testing potential for this payload.

4.2.6 Final design

Once all the subsystems and payloads have been distributed in the units, the structural design of the CubeSat can be concluded. So that, we can proceed to obtain the final dimensions, weights, inertia, etc.

- **Final mass and envelope**

With all the subsystems integrated and all the structure assembled we can obtain the mass and the envelope dimensions. The reference axes used are the following: positive Z pointing to Nadir, positive X in the direction of flight speed and Y axis forming a right-hand trihedron (pointing to Sun).

This data are shown in Table 4.10a. Seeing this values we can confirm that we match the weight and maximum envelope requirements.

- **Center of Mass**

This point is going to be related to the center of mass of the main structure. The CoM coordinates can be extracted directly from the CAD program used and have been written in Table 4.10b.

Now we can verify that the CoM is inside the envelope fixed in [1].

- **Inertia matrix**

As it has been done with the center of mass, the inertia matrix of the CubeSat is extracted from the CAD program. This inertia are referred to the satellite's CoM. This values can be seen in Table 4.10c

Table 4.10: Final satellite properties

(a) Mass & Center of Mass coordinates				(b) Center of Mass coordinates		
mass [kg]	x [mm]	y [mm]	z [mm]	x [mm]	y [mm]	z [mm]
6,923	238.5	101	334	-3.35	-8.45	3.75

(c) Inertia matrix			
mass [kg]	x [mm]	y [mm]	z [mm]
6,923	238.5	101	334

The final design, already with the surfaces of the materials selected by the power subsystem, can be seen as it is ejected from the dispenser in Figure 4.15.

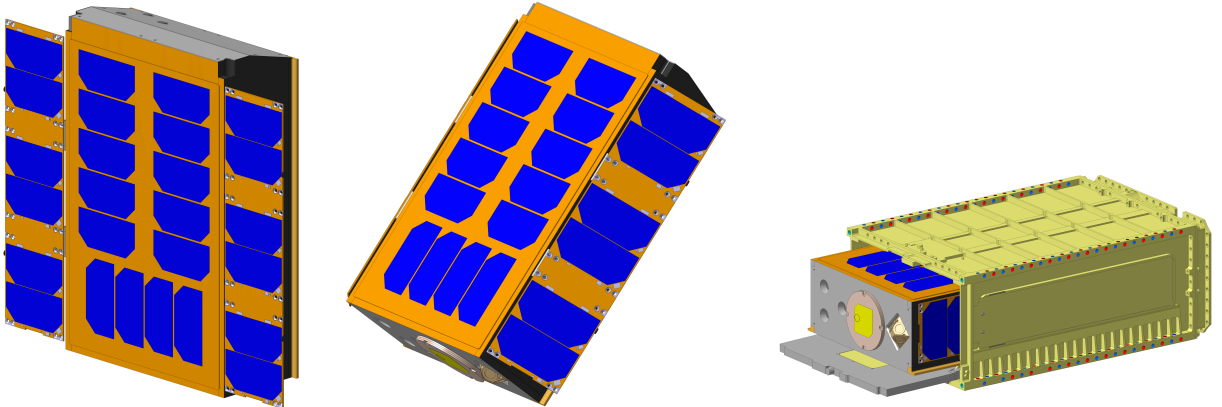


Figure 4.15: Final design CubeSat

4.3 Thermal Control Subsystem

When designing a satellite, the temperature range of each instrument must be taken into consideration, ensuring that the thermal conditions of the satellite's life will be suitable for the on-board equipment. To achieve that, the thermal control subsystem is implemented.

Heat transfer is assort into three different processes: Convection, conduction and radiation. Due to being in microgravity, natural convection seldom occurs. Hence, heat exchange between the environment and the satellite is achieved via radiation, mainly from the Sun and albedo from Earth (reflected sunlight). Conduction also takes place in the satellite, when two or more different physical interfaces, at distinct temperatures, are in contact. In addition, heat sources within the satellite, such as power dissipation, will modify the thermal equilibrium.

To counteract the environmental and internal heat sources, as to keep the thermal equilibrium of the satellite in a specific range, active and passive solutions will be taken into account:

- Passive solutions: They do not require power to function. Some of them are coatings for the satellite's structure such as Kapton, or covers, such as MLI or radiators.
- Active solutions: They require power to function. The most common are heaters, electrical, chemical or nuclear, to increase the satellite's temperature.

4.3.1 Requirements

The overall requirement of this subsystem is to keep the instrumentation within its ranges of working temperatures, during their operation, and survival temperatures, during the satellite's on-orbit life.

Regarding the mission requirements, the only explicit requirement for this subsystem defines the radiometers' working temperature range, from 11 °C to 21 °C, being 16 °C the optimum temperature for operation, and their working range, between -20 °C and 50 °C.

Implicitly, the SSO defined for the mission constrains the thermal environment of the satellite. Furthermore, the radiometers require to be pointing to Nadir and Zenith, constraining their integration surfaces to be facing the Earth and deep space respectively.

Temperature ranges for each subsystem, concerning their operational and survival requisites, can be found in Table 4.11, provided from the subsystem's equipment.

Table 4.11: Temperature ranges for the on-board components selected for the mission.

Subsystem	Component	Operational (°C)	Survival (°C)
Communications	Antenna	-20 to 50	—
	Transciever	-40 to 70	—
ADCS	Sun Sensor	-40 to 70	—
	Magnetometer	-40 to 70	—
	IMU	-40 to 85	—
	GPS	-30 to 70	—
	Magnetorquer	-40 to 70	—
	Reaction Wheel	—	—
Power	Solar cells	-55 to 125	—
	Batteries	-40 to 70	—
Payload	Radiometers	11 to 21	-20 to 50

4.3.2 Preliminary model

The SSO (6 AM) described by the satellite will condition the thermal control and environment of the satellite. Within the space environment and as mentioned before, different heat sources must be considered, them being:

- Sun's radiation: Due to the Sun's temperature (5672 K). The nominal value of the direct solar incident energy on a surface, normal to a line from the Sun, is called solar constant, whose value is $S = 1366.1 \text{ W/m}^2$, according to ISO 21348 (2007) [7].
- Earth's radiation: Heat exchange with the satellite due to the Earth's temperature of 300 K.
- Earth's albedo: Accounts for the sunlight reflected by the Earth. Modelled as 30% the value of the solar constant.
- Deep space's radiation: Heat exchange with the satellite due to the Space's temperature of 3 K [8].
- Internal heat losses of the satellite: For this 6U satellite, overall losses of 20 W have been considered, to account for all the on-board equipment [8].

As the orbit is sun-synchronous of 6 AM, the local vertical of the satellite and the sun vector remain mostly perpendicular, during the on-orbit life. Hence, the albedo effect can be neglected for this preliminary study in favour of simplicity [10]. Likewise, the inclination of the Zenith-pointing face of the satellite has not be taken into consideration.

As the attitude control subsystem constrains satellite into a fixed orientation, the thermal control has been designed consequently, focusing on a preliminary steady-temperature study.

To assess the proposed thermal environment of the mission, a one-node model of the satellite was defined. After its study, the satellite was broken down into a three-node model, as to provide more accurate results. In this section both of them will be presented and discussed.

Additionally, in the Table 4.12, several different coatings that will be used in the models are shown. Coatings named "black" and "white" refer to anodized treatments for aluminium, as specified in ECSS-E-30 Part 8A.

Table 4.12: Materials and coatings commonly studied for thermal control [12].

Coating or material	ε	α
Solar cells	0.84	0.75
Aluminium (Raw)	0.30	0.13
Kapton	0.03	0.13
Aluminized Kapton	0.34	0.25
Black	0.87	0.95
White	0.88	0.23

4.3.2.1 One-Node Approximation

The first approximation to compute the temperature of the satellite is to design a one-node model. Then, all the components of the satellite will be at the same temperature, regardless of their position or composition.

The model's behaviour is summarized in Equation 4.8 where the solar panels' contribution is weighted via the efficiency of the cells (from electrical power subsystem), considering the solar panel surface to be completely cover with solar cells. Besides, the effect of an eclipse has been studied (cold case), as to provide a complete thermal study of the critical cases. This will give an estimate result, to ensure proper functioning, if the orbit altitude is modified in future design iterations. The materials and coatings, implemented on the satellite's external surfaces, for this model can be found in Table 4.13. Figures 4.16 and 4.17 show the faces nomenclature, being SP the solar panel face.

Table 4.13: Materials and coatings selected for the one-node model.

Face	Coating or material
SP	Solar cells
Face 2	Black
Face 3	Black
Face 4	Black
Face 5	Black
Face 6	Black

$$S\alpha_{SP}A_{SP}(1 - \eta_{SP}) + \dot{Q}_{internal} = \sigma\varepsilon_{SP}A_{SP}T^4 + \sigma\varepsilon_2A_2(T^4 - T_0^4) + \sigma\varepsilon_3A_3(T^4 - T_t^4) + \sigma\varepsilon_4A_4(T^4 - T_0^4) + \sigma\varepsilon_5A_5(T^4 - T_0^4) + \sigma\varepsilon_6A_6(T^4 - T_0^4) \quad (4.8)$$

The results are summarized in Table 4.14, where the solar constant has been studied under its maximum, minimum and average values [7]. This variation has no effect on the cold case as the Sun is eclipsed by the Earth.

Table 4.14: Temperatures for the one-node analysis for hot and cold cases.

	Solar constant (W/m ²)	T Node (°C)
Hot case	1412.9	18.365
	1366.1	16.502
	1321.1	14.675
Cold case		-70.096

The results obtained for the hot case scenario, falls within the specified ranges of operational temperature for the components of the satellite, being the temperature value for the average solar constant near to the optimal working temperature of the radiometers. Regarding the eclipse results (cold case), the temperature exceeds the operational range of all the instruments, including the radiometers. Hence, a more complex model has been implemented to provide more accurate results.

4.3.2.2 Three-Node Approximation

To provide a more accurate solution and to get additional information regarding the state of the satellite, a new model with three nodes is developed and schematized in Figures 4.16 and 4.17. In this case, each node is defined as:

- First node: Solar panel's surface. They receive all solar energy and radiate it to the satellite.
- Second node: Face in contact with the solar panel. Under the hypothesis that conductive heat has been insulated, only radiation remains.
- Third node: The remaining faces of the satellite. Temperature is assumed equal, as it has reached equilibrium through conduction and internal radiation.

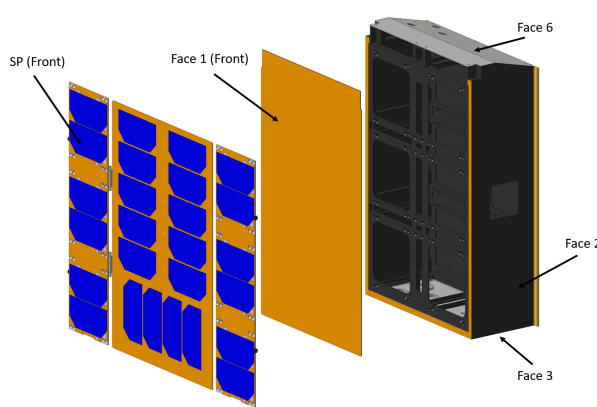


Figure 4.16: Three-Node distribution front diagram.

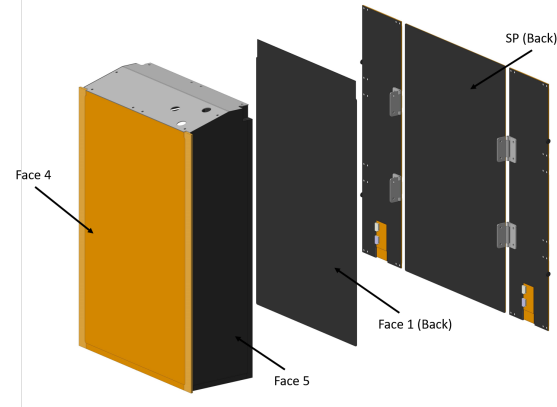


Figure 4.17: Three-Node distribution back diagram.

For this model, new faces and coatings have been implemented. Each material is indicated in Table 4.15.

Table 4.15: Materials and coatings selected for the three-nodes model.

Face	Coating or material
SP (Front)	Solar cells
SP (Back)	Black
Face 1 (Front)	Kapton
Face 1 (Back)	Black
Face 2	Black
Face 3	Aluminized Kapton
Face 4	Kapton
Face 5	Black
Face 6	Aluminized Kapton

With these, the model is closer to what will happen in reality. The system of equations proposed below for the model, covers the equilibrium temperature of the three nodes. As the satellite implements two deployable solar panels, view factors have been defined to account for the heat radiated from them to faces 2 and 5 and vice versa.

$$S\alpha_{SP}A_{SP}(1 - \eta_{SP}) = \sigma\varepsilon_{SP}A_{SP}T_1^4 + \sigma\varepsilon_{SP,back}A_1(T_1^4 - T_2^4) + \sigma\varepsilon_{SP,back}F_{1,3}A_{LP}(T_1^4 - T_3^4) + \sigma\varepsilon_{SP,back}(1 - F_{1,3})A_{LP}(T_1^4 - T_0^4) \quad (4.9)$$

$$\sigma\varepsilon_{1a}A_1(T_1^4 - T_2^4) = \sigma\varepsilon_{1b}A_1(T_2^4 - T_3^4) \quad (4.10)$$

$$\dot{Q}_{internal} = \sigma\varepsilon_{1b}A_1(T_3^4 - T_2^4) + \sigma\varepsilon_2A_2[(T_3^4 - T_1^4)F_{3,1} + (T_3^4 - T_0^4)(1 - F_{3,1})] + \sigma\varepsilon_3A_3(T_3^4 - T_t^4) + \sigma\varepsilon_4A_4(T_3^4 - T_0^4) + \sigma\varepsilon_5A_5[(T_3^4 - T_1^4)F_{3,1} + (T_3^4 - T_0^4)(1 - F_{3,1})] + \sigma\varepsilon_6A_6(T_3^4 - T_0^4) \quad (4.11)$$

The results obtained for this model, following the procedures of the previous one-node model, are presented in Tables 4.16 and 4.17.

Table 4.16: Temperatures for the tree-node analysis under different solar constant values (Hot case).

	$S = 1412.9 \text{ (W/m}^2)$	$S = 1366.1 \text{ (W/m}^2)$	$S = 1321.1 \text{ (W/m}^2)$
T Node 1 (°C)	41.792	39.611	37.469
T Node 2 (°C)	17.255	16.855	16.469
T Node 3 (°C)	16.291	15.969	15.659

Table 4.17: Temperatures for the tree-node analysis under eclipse conditions (Cold case).

	No sun incidence
T Node 1 (°C)	-70.257
T Node 2 (°C)	43.637
T Node 3 (°C)	6.057

The results obtained for the inner temperature of the satellite, falls within the specified operational ranges for the on-board equipment, for the hot case. Regarding the cold case, the inner temperature meets the survival range of the radiometers and the operational range of the other instrumentation. Despite this, during an hypothetical eclipse period, the solar panels reach an value outside their operational range, that could be able to damage them.

4.3.3 Discussion of results

In light of the results for both models, a solution must be chosen to provide the preliminary thermal control design. Despite both models reaching similar ranges of inner temperature for the satellite, the tree-node model provides greater accuracy, as it is more discretized.

One of the main advantages of the three-node model is that, the solar panels, are isolated form the satellite's main structure, providing their temperature. This information allows for more precise definition of the power subsystem as the efficiency of the solar panels depend on their cells' temperature.

For the cold case, in both models, a temperature close to -70 °C is reached but, as the three-node model highlights, this temperature corresponds to the solar panels, showing that the satellite's inter temperature meets the thermal constrains. Even thought, as mentioned before, the temperature reached by the solar panels outreaches their operational range, endangering them. Despite this, the solar panels will never reach this temperature, as LEO average eclipse period is close to 20 minutes [11], not enough time to decrease their temperature from 40°C to -70°C.

To summarize, the **three-node model has been selected** due to its precision, even though several simplifications have been implemented, such as considering conductive coupling and optimal distribution of the instruments inside the satellite, to balance the inner temperature gradients, no albedo effect, etc. The target temperature has been reached without active heating, so it is energy-saving and cost-efficient. In followings reviews, and with additional data from other subsystems and tools, a more complex analysis should be performed to validate this results.

4.4 Attitude Determination and Control Subsystem

The Attitude Determination and Control System (ADCS) is in charge of determining, stabilising, and controlling the orientation of the spacecraft. For this purpose, it uses sensors to obtain information about position and attitude, as well as actuators to control the desired orientation.

For the ADCS design, the needs imposed by the scientific payload shall be considered. Thus, the mission requirements relevant to this system must be identified in order to analyse their impact on the proper design of this subsystem. These requirements are: **R-090**, **R-100**, **R-150**, **R-160**, **R-170**, and **R-180**; which involve a specific pointing direction, as well as attitude and position knowledge with a restricted accuracy. Together with that, there are several mission constraints affecting the ADCS design, namely size, mass, power, volume, space environment,

lifetime, and cost. All these aspects will be taken into account in order to provide a suitable ADCS for this mission.

Having established requirements and constraints, the process of the ADCS design will begin with the estimation of the disturbances, so as to know the main disturbances the vehicle will encounter during its lifetime and their magnitude. This will depend on the space environment, which in turn is determined by the operational orbit. Therefore, the orbital parameters provided by the Mission Analysis subsystem will define the torque magnitude that actuators must compensate for.

The attitude control method is then selected. After that, a research on the ADCS used for similar missions is conducted, in order to get acquainted with commonly used components and their applicability in 6U CubeSats for Earth Observation missions in LEO orbits. Next, different possibilities for the ADCS definition are weighed by means of a trade-off analysis, in which each component's suitability for MARTINLARA mission is thoroughly assessed. Conclusions stated, this step is followed by the hardware selection. Finally, the mission operation modes are described.

The interactions that this subsystem will have with other subsystems are illustrated in the Figure below.

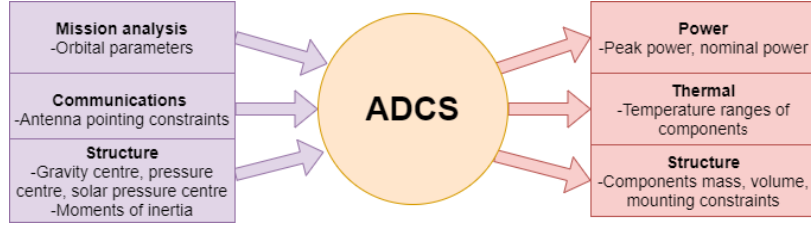


Figure 4.18: ADCS trades with other subsystems.

4.4.1 Disturbance sizing

The ADCS is responsible for measuring and counteracting the effect of the external and internal disturbances that the satellite will encounter along its orbital trajectory. These will have an impact on the spacecraft's attitude motion and, therefore, the mission's success will rely on the ADCS being able to counter such disturbances, which in turn, will require their magnitudes to be quantified. Since the ADCS must be capable of handling the attitude motion of the satellite at all times, the most extreme cases will be considered, and since most of the disturbances decrease with altitude, the values of the periapsis of the orbit will be used for the estimations. Furthermore, the spacecraft's total disturbance torque, which will be the sum of all the disturbances, will be estimated as it will be the key dimensioning factor for the system.

Generally, considerably more weight is assigned to the analysis of the external, rather than the internal, disturbances as these have a continuous effect on the angular momentum of the satellite. Such disturbances, in the orbit chosen for the MARTINLARA CubeSat, are mainly originated from four phenomena: the gravity gradient torque, the solar radiation pressure (SRP), which is dependant on the solar activity, the aerodynamic drag torque, which is the most significant disturbance for orbits below 500 km, and the residual magnetic dipole torque of the spacecraft. This information is summarised in Table 4.18 below.

Table 4.18: External Disturbance Torques

Source	Dependence on earth distance	Region of space where dominant
Gravity Gradient	$1/r^3$	500 - 35 000 km
Solar Radiation	Independent	Interplanetary space
Aerodynamic	$e^{-\alpha r}$	< 500 km
Magnetic	$1/r^3$	500 - 35 000 km

Internal disturbances, on the other hand, are originated from the satellite components, resulting in torques due to the reaction wheel friction and electromotive force, rotating machinery or liquid slosh, among other factors. As the MARTINLARA satellite will have minimal moving parts and no fuel deposit, the effect of such disturbances will be negligible in a first analysis. Consequently, this section will focus primarily on the external disturbances that the

satellite will encounter along its orbital path. For the sake of brevity, the equations and the terms involved for the estimation of each disturbance torque are presented in the Appendix B.

4.4.1.1 Disturbance Torques Estimation

The results of the disturbance quantification analysis are presented in this subsection. As seen in Table 4.19, the total torque that the ADCS is estimated to encounter is $19.7 \text{ mN} \cdot \text{mm}$.

Table 4.19: Estimated Disturbance Torques

Disturbance Torque	Torque [$\text{mN} \cdot \text{mm}$]
Gravity Gradient Torque	$3.93 \cdot 10^{-4}$
Solar Radiation Pressure Torque	$4.47 \cdot 10^{-3}$
Aerodynamic Drag Torque	2.19×10^{-3}
Magnetic Torque	19.6
Total Torque	19.7

It can be seen that the major contributor to the external disturbances is the magnetic torque, while the effect of the gravity gradient torque, SRP torque and aerodynamic torque is almost negligible. This is consistent with the theory, as at the chosen orbit the atmosphere is almost at a vacuum and hence the aerodynamic drag is minimum, and due to the symmetry of the satellite and the location of the centre of gravity, the SRP is minimum.

Nevertheless, it must be noted that due to the early design stages at which the MARTINLARA mission is currently at, these numbers are subject to change and some parameters used are rough estimates. Therefore, further analysis is needed in order to validate the results, which is out of the scope of this document.

4.4.2 Spacecraft control selection

Having stated the ADCS requirements and the external disturbances acting on the spacecraft, the attitude control method must be selected. Three different techniques will be evaluated: gravity gradient, spin-stabilisation and 3-axis zero momentum stabilisation.

- **Gravity gradient stabilisation** can be useful for coarse pointing ($\sim 5^\circ$) around the nadir axis. Considering the accuracy requirements imposed, and the fact that only one axis is stabilised, this control scheme is rejected.
- **Spin stabilisation** is directly discarded owing to mission requirement R-100 and the solution adopted to accomplish it.
- **Zero momentum stabilisation** is the option selected, which can provide higher accuracy and a complete control of the vehicle.

4.4.3 ADCS heritage designs

This section covers the ADCS configurations used by similar satellites in order to obtain information on flight-proven components that are used for 6U CubeSats. The information that was gathered through the heritage design analysis is presented in the tables below.

Table 4.20: ADCS used in similar missions.

	CubeSTAR	ASTERIA	TEMPEST-D	GTOSat
CubeSat Units	3U	6U	6U	6U
Control Axis	3-axis	3-axis	3-axis	3-axis
Pointing Accuracy	$< \pm 10^\circ$	N/A	$\pm 0.007^\circ$	$< \pm 1^\circ$
Attitude Determination	Sun Sensors, Gyroscopes and Magnetometers	Sun Sensors, IMU, Star-tracker and Magnetometer	Sun Sensors, IMU, Star-tracker, Magnetometer, GPS/GNSS	Sun Sensors, IMU, Star-tracker, Magnetometers
Attitude Control	Magnetorquers	Reaction Wheels, Magnetorquers	Reaction Wheels, Magnetorquers	Reaction Wheels, Magnetorquers
Orbit	Near Polar LEO	LEO	LEO	GTO

4.4.4 Trade-off analysis

Prior to the selection of components, a trade-off analysis is provided for choosing the most suitable options for this mission. According to the mission requirements, accuracy will be a determining factor in this trade-off, alongside with the weight, size, power consumption and reliability of the components. Furthermore, the magnitudes of the disturbance torques will be considered to select an actuator system that is able to counteract them.

4.4.4.1 Attitude determination

There are two categories of sensors: reference sensors and inertial sensors. The latter can take continuous measurements as they are not interrupted by eclipses, but they require attitude or calibration corrections from reference sensors. Usually, a combination of both types of sensors is applied. The sensors that will be analysed in following are: sun sensors, earth sensors, star trackers, gyros, magnetometers, and GNSS/GPS.

Sun sensors provide good attitude reference when orbiting Earth, due to the Sun's high luminosity and small apparent size. These sensors are able to provide an appropriate accuracy for this mission, with the drawback that measurements may be ambiguous if the incoming sunlight lies along the generatrix of the cone of vision. Nonetheless, this issue is successfully addressed by positioning one sun sensor on each face of the satellite, i.e., six sun sensors.

Besides, sun sensors are particularly interesting for this mission since there are constraints regarding the space-craft position relative to the Sun. These sensors would play a double role: providing attitude determination and verifying that the Sun incidence in the vehicle is correct. Therefore, their application will definitely be considered for the components selection.

Earth sensors take Earth's horizon as a reference direction to determine the spacecraft orientation. This type of sensors are cheap, and their performance is enhanced in LEO, but they usually provide poor accuracy for CubeSat applications. Therefore, they are considered to be insufficient to fulfil the requirements imposed.

Star trackers are the most accurate sensors. However, they are more expensive and imply more complexity. They demand additional requirements regarding other satellite systems, such as mechanical and thermal stability, computers and data handling, software, etc. Their use would be considered for interplanetary missions or higher orbits where other sensors such as magnetometers can not be used.

As **magnetometers** operate with the Earth's magnetic field, their performance depends on their distance to Earth. For this reason, these sensors are especially effective in LEO. Additionally, their weight, size, simplicity, and price make these sensors an attractive choice for attitude determination. However, two aspects shall be taken into account. The first one is that the Earth's magnetic field has several disturbances and does not act the same depending on the region where the satellite is at. Consequently, magnetometers provide coarse measurements and they are commonly used in combination with other sensors. The second aspect is that these sensors are very sensitive to the noise that could be generated by other subsystems, so it is necessary to locate them as furthest as possible from any noise source.

Gyros are often used when high performances are required. They are independent of the environment and can support the accuracy of a star tracker, but these sensors tend to drift. That is why they are often used in combination with accelerometers, conforming an IMU, which allows authentic measurements of the spacecraft's orientation and position. The use of gyro-rate sensors also allows a suitable control the angular rate of the spacecraft. Differentiating angular position outputs from other sensors to get the angular rates can lead to noisy results, which would affect the stability and pointing of the vehicle.

The aforementioned sensors provide information regarding the attitude of the satellite, but the position would remain unknown. **GNSS/GPS** signals can be used both for position and attitude determination.

4.4.4.2 Attitude orientation

Actuators must be able to counteract external disturbances with the accuracy required so as to maintain the appropriate orientation. They can also be divided into inertial and non-inertial types. Among inertial types, only reaction wheels will be considered. Momentum wheels are discarded because of having selected the zero momentum

controlling method, and Control Moment Gyroscopes (CMG) are unnecessary for such a small vehicle. Non-inertial actuators are thrusters and magnetorquers.

Reaction wheels are widely used for fine tuning and accurate pointing. However, they require the implementation of another actuator to help desaturate them. Magnetorquers or thrusters are often used to dump some of the momentum. A minimum of three non-co-planar wheels are required for full three-axis control. In order to reduce the risk of failure, a fourth redundant wheel is usually added in a skewed configuration. It is also possible to adopt a configuration with four wheels off-axis, in which redundancy is maximised.

The use of **thrusters** is especially interesting for either interplanetary missions or very high orbits around Earth, where the magnetic field is too weak. For this mission, these actuators involve an unnecessary increase of mass, price, volume, and complexity. Therefore, their implementation is rejected.

Magnetorquers are usually applied in LEO for the same reason as magnetometers. Also, their utility decreases with altitude as the magnetic field is weaker. These actuators do not require any propellant, demand very limited power levels, and have an unlimited lifetime, as well as simplicity and no moving parts. Usually, three magnetorquers are used for either coarse attitude control or angular momentum unloading.

One feature that needs to be paid attention to is that magnetorquers cannot produce a torque component about the local field direction. In a polar orbit, this issue does not imply any limitation in the attitude control as any direction can be achieved at some point around the orbit. Equatorial orbits may encounter some limitations, though, because the field lines are always in the same direction (north-south). Nevertheless, as MARTINLARA mission orbit is very close to polar, this effect is considered negligible.

4.4.5 ADCS components

4.4.5.1 Component Selection

The actuators that will be used are **reaction wheels** for fine pointing accuracy and **magnetorquers** for the momentum unloading. Therefore, **magnetometers** are also required. Since these sensors provide poor accuracy, they will be combined with **sun sensors**. Inertial sensors will also be included by means of an **IMU** to directly measure the spacecraft angular rates and accelerations. Finally, a **GNSS/GPS** will be implemented for position determination. The list of these components is showed on Table 4.21.

Table 4.21: ADCS components listing. (*) Both magnetometer and magnetorquer belong to the same component.

ADCS Component		Name	Supplier	Quantity
SENSORS	Sun sensor	FSS100	Tensor Tech	6
	Magnetometer	iMTQ (*)	ISIS	1 (3-axis)
	IMU	STIM300	Sensonor	1
	GPS	OEM7600	NovAtel	1
ACTUATORS	Magnetorquer	iMTQ (*)	ISIS	3
	Reaction Wheel	RWP050	Blue Canyon	4

It must be noted that components that met the requirements but for which the data-sheet was not publicly available, were avoided.

Sensors Regarding the number of components chosen, and owing to the reasons commented in the trade-off, six sun sensors will be required as well as one 3-axis magnetometer. Besides, the Inertial Measurement Unit (IMU) consists of three MEMS gyros, three accelerometers and three inclinometers.

As seen in Table 4.22, the **R-170** requirement is already met with the sun sensor, but the IMU fulfils the goal accuracy. Regarding the GPS position accuracy [17], it has been specified the horizontal positioning. Vertical

positioning is typically determined with 1.7 times the horizontal accuracy, so in any case both measurements are suitable enough to accomplish requirement **R-180**.

Table 4.22: Performance details of the selected sensors [18], [21], [20], [19].

Sensor	Name	Accuracy
Sun Sensor	FSS100	0.1°
Magnetometer	iMTQ	< 3 μT
IMU	STIM300	0.02°
GPS/GNSS	GPS Patch Antenna	1.5 m RMS

Actuators The reaction wheels that have been chosen for the system, the RWP050 by Blue Canyon, provide a sufficient maximum torque performance that would be able to counteract the estimated total disturbance torque with a FoS of 2.5. These have been used in several missions by NASA and ESA alike, like the Asteria or Tempest-D CubeSats described in the heritage design section. Moreover, four of these wheels have been selected as to provide redundancy to this system in order to reduce the risk **AD-001** (see Section 5).

Since the magnetorquers will mainly be used for desaturating the reaction wheels, and their performance is not as crucial, some trade-offs can be made in order to minimise the volume, mass and power consumption of the system. Therefore, the chosen magnetorquers are integrated in the same board as the magnetometers which greatly reduces the volume taken, as well as it makes the integration easier. Further details are provided in Table 4.23.

Table 4.23: Performance details of the selected actuators. The information is provided for a single actuator [21], [22].

Actuator	Name	Performance
Reaction Wheel	RWP50	Max torque: 0.007 N·m
Magnetorquer	iMTQ	Nominal actuation: 0.2 Am^2

4.4.5.2 System Budgets - SWaP

Table 4.24 shows the System Weights and Power table for the chosen ADCS system.

Table 4.24: SWaP [18], [20], [19], [22], [21].

Component	Volume [cm^3]	Weight [kg]	Peak Power [W]
Reaction Wheels (x4)	84.1	0.240	1.00
Magnetorquer board	146.9	0.20	1.15
Sun Sensors (x6)	N/A	0.010	0.10
IMU	37.2	0.055	1.00
GPS/GNSS	73.5	0.016	0.03
ADCS System	900	1.29	3.90

4.4.6 ADCS Mission Operation Modes

This section covers the mission operation modes for which the MARTINLARA satellite is configured. These will be used for different purposes and at different times throughout the mission.

4.4.6.1 Safe-Mode

In the Safe-Mode the satellite will start booting up and begin to send telemetry back to Earth, it will have access to the data from the housekeeping sensors, together with the received commands. At this point the actuators and sensors are turned off.

Table 4.25: Safe-Mode

ADCS Booting up	Yes
ADCS is sending telemetry	Yes
ADCS is receiving commands	Yes
Available Data for ADCS	Housekeeping sensors
Actuators for AC	Off
Sensors for AD	Off

4.4.6.2 Science Mode

In this mode all the sensors will be active as to provide the satellite with an accuracy in attitude determination that complies with the mission requirements. Similarly, the reaction wheels will be on as to provide control over the satellite attitude motion that is compliant with the mission requirements.

Table 4.26: Science Mode

ADCS is receiving commands	Yes
ADCS is sending telemetry	Yes
Available Data for ADCS	GPS, IMU, Sun sensors, magnetometer (3-axis)
Actuators for AC	On
Sensors for AD	On

4.4.6.3 System Maintenance Mode

This mode will be active when it is necessary to use the magnetorquers to desaturate the reaction wheels.

Table 4.27: System Maintenance Mode

ADCS is receiving commands	Yes
ADCS is sending telemetry	Yes
Available Data for ADCS	GPS, IMU, Sun sensors, magnetometer (3-axis)
Actuators for AC	Magnetorquers On, Reaction Wheels Off
Sensors for AD	On

4.5 Command and Data Handling

Once the structure is designed, and before starting to define the position of all elements, a computer for the on-board data handling must be selected. The computer selected is the ISIS On Board Computer (iOBC) (see Figure 4.19), a flight qualified, high performance processing unit.

This computer is able to fulfill all of the memory needs provided by the communications subsystem calculations, providing 2 x 2GB high-reliability SD cards for fail-safe data storage (up to 32 GB on request) or 2x any size standard SD cards.

Once selected, some of its properties will be important for the satellite design:

- Operating Temperature: -25 degC to +65 degC
- Power Supply: 3.3V
- Dimension: 96 x 90 x 12.4 [mm] (including FM daughter board)
- Mass: 94g mainboard only, 100g with EM daughter board
- Power Consumption: 400mW average



Figure 4.19: ISIS On Board Computer.

4.6 Communication Subsystem

The complete definition of the communication subsystem has been divided into the following four sections. The first one, Preliminary Link Design, will provide general information about the requirements of the subsystem. Following, the Ground Station is selected and its main characteristics are defined. The third section, Satellite Design, deals about the antenna and transceiver on board the satellite. Finally, in order to check that the data is transferred properly, in Link Budget Design section the system link margin is verified.

4.6.1 Preliminary Link Design

Firstly, the orbit parameters and requirements must be known. The satellite is designed to operate in a sun-synchronous orbit at 500 km of altitude, as seen in previous sections. Considering the main objectives of the mission, the satellite must be able to transmit the data acquired to a ground station. In order to ensure this transmission, a data rate has been estimated based on the fact that all the information transmitted will be only data files. The selected bit rate can be consulted on Table 4.28.

Furthermore, the data downlink and uplink will be performed via S-band, since it is one of the most common bands used in satellites communications. This band has a low frequency ranges and can be used for long distance communications.

Table 4.28: Preliminary Link Design

Orbit altitude	500 km
Bit Rate	20 Kbps
Band	S-band

4.6.2 Ground Station

Based on the mission requirements, the ground station selected for this mission is Kiruna, which belongs to the core ESA-owned stations. This ground station hosts an antenna with reception and transmission in S-band, as well as the capability of autotracking the satellite. Its coordinates can be found on Table 4.29. Kiruna's antenna, with 15 m of diameter, has a transmitter power of 54.8 dBm and an uplink and downlink gain of 46 dBi and 48.6 dBi respectively.

Table 4.29: Kiruna Ground Station [23]

GS Coordinates	Antenna gain	Antenna diameter	Transmitter power
67° 51' 25,66" N 20° 57' 51,57" E	Uplink: 46 dBi	15 m	54,8 dBm
	Downlink: 48,6 dBi		

4.6.3 Satellite Design

Regarding the instruments onboard the satellite, an antenna and the instruments in charge of receiving and transmitting data shall be defined.

4.6.3.1 Antenna

The selected antenna is the ISIS S-band patch antenna, which is a compact and low mass element suitable for any CubeSat platform. It is shown in Figure 4.20, and its main characteristics are presented in Table 4.30.

Table 4.30: Antenna [24]

Gain	6,5 dBi
Half Power beam Width	100°
Pointing error	10°
Mass	50 g
Operational Temperature	-20 - 50 °C
Diameter	80 mm

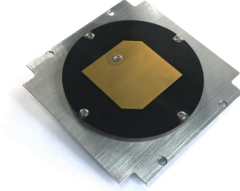


Figure 4.20: ISIS S-band patch antenna [24]

4.6.3.2 Transceiver

Instead of carrying a receiver and a transmitter, the satellite will use a transceiver which will allow both, data transmission and reception. Two transceivers have been considered, a CubeSat S-Band Transceiver of the company NanoAvionics, shown in Figure 4.21, and the ISIS S-band Transceiver.

Considering that the data will be transmitted and received successfully with both of them, the ISIS transceiver has been discarded because it consumes up to 13 W, while the first one consumes 6,5 W. Thus, the main features of the selected transceiver can be consulted on Table 4.31.

Table 4.31: Transceiver [25]

Modulation	GMSK
Transmit Frequency	2200-2290 Mhz
Transmit Power	30 dBm
Receive Frequency	2025-2110 Mhz
Power consumption	6.5 W
Operating Temperature	-40 - 70 °C
Input Voltage	5 - 40 V
Dimensions	93 x 87.2 x 17 mm
Mass	0.192 kg

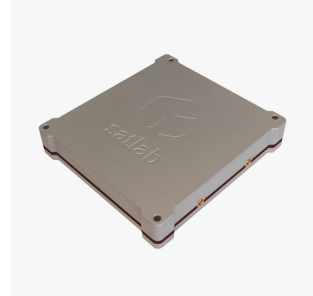


Figure 4.21: NanoAvionics CubeSat S-Band Transceiver [25]

4.6.4 Link Budget Design

Finally, in order to ensure that the data transmitted and received is not lost during its emission, a link budget design, shown in Table 4.32, is developed.

Table 4.32: Link Budget Design

	Uplink	Downlink
Frequency [GHz]	2.07	2.250
Overall Losses [dB]	167	166.5
EIRP [dBW]	99.8	36
System Noise Temperature (T) [K]	614	93
Figure of merit (G_{ant}/T) [dB/K]	-21.38	28.92
Carrier to Noise Power Density (C/N_0) [dBHz]	80.99	67.51
E_b/N_0 [dB]	37.98	24.5
$(E_b/N_0)_{req}$ [dB]	9.59	9.59
System Link Margin [dB]	28.39	12.91

It can be mentioned that the operation frequencies belong to the S-band range, and they are covered by the frequencies accepted by the antenna and the transceiver. The uplink noise temperature is a theoretical estimation [26], while the downlink noise temperature is characteristic of the ground station [23].

Regarding to E_b/N_0 parameter, which is defined as the energy per bit (E_b) to the spectral noise density (N_0), it refers to the basic measure of how strong the signal is. Thus, it is essential to analyse the system link margin, which is the difference between E_b/N_0 obtained and the required value for a probability of bit error (BER) of 10^{-5} . This system link margin should be positive and as high as possible, because the probability of bit error decreases while E_b/N_0 increases, as shown in Figure 4.22. The value of this parameter, shown in Table 4.32, is positive and it provides sufficient margin for a correct operation.

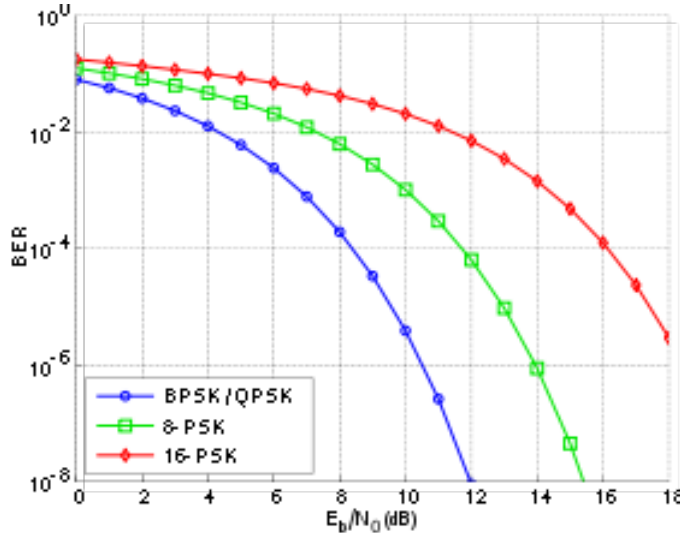


Figure 4.22: NanoAvionics CubeSat S-Band Transceiver [27]

Hence, after checking these values, it can be concluded that the configuration presented in this section is suitable to perform the mission properly.

4.7 Electrical Power Subsystem

The electrical power subsystem (EPS) provides, stores, distributes and control spacecraft electrical power, which is, along with mass, the second critical resource in the design of a spacecraft. In order to size each component of this subsystem it is necessary to estimate the power requirements of each of the subsystems of the mission, analysing different operating modes associated with different stages of the mission. Before doing that an overview of the calculations needed for selecting the power source as well as the energy storage will be given.

4.7.1 Power Source

Photovoltaic solar cells, which convert incident solar radiation directly to electrical energy, are the most common power source, therefore this section is focused in the design of this element. The main objective of this design is to obtain the solar array area, A_{sa} , required to support the spacecraft power requirements, which is given by

$$A_{sa} = \frac{P_{sa}}{P_{EOL}} \quad (4.12)$$

where P_{sa} is the total power that the solar array must provide during daylight, and P_{EOL} is the electrical power load for mission operations at the end-of-life given by

$$P_{EOL} = P_{BOL}L_d \quad (4.13)$$

Which takes into consideration the effects of degradation during its lifetime, L_d , on the electrical power load for mission operation at the beginning-of-life, P_{BOL} . Life degradation is caused by thermal cycling, micrometeorite strikes, plume impingement from thrusters, and material outgassing for the duration of the mission [9]. L_d depends on the degradation per year, c , which has been considered to be 2.75% for Gallium Arsenide cells in LEO [26]. It also depends on the satellite lifetime, t_f , which in this case is less than a year.

$$L_d = (1 - c)^{t_f} \quad (4.14)$$

It is also necessary to take into account the inherent degradation of the cells, I_d . This parameter considers losses due to design inefficiencies, shadowing and temperature variations [9], which result in the assembled solar array being less efficient than the single cells. Its values might vary from 0.49 to 0.88, in this particular mission it has been considered to be 0.77.

The efficiency of the solar cells, η , must also be defined. Due to the demanding power requirements of this mission, gallium arsenide cells have been selected which for this preliminary estimation have been considered to have a 28% efficiency.

Once these parameters have been defined it is possible to compute the power load for mission operation at the beginning-of-life given by

$$P_{BOL} = P_{SUN}\eta I_d \cos(\theta) \quad (4.15)$$

where P_{SUN} is the solar illumination intensity which depends on the distance between the Sun and the satellite, in this case it has been given a constant value of 1367W/m², although it could value between 1321.1 and 1412.9W/m² during the year.

And θ is the Sun incidence angle, which has been measured as the angle between the vector normal to the surface of the array and the Sun line resulting in a maximum angle of 16.4° and a minimum angle of 0° which is the angle formed in the most favourable case, when the Sun rays are perpendicular to the solar array surface, allowing to get maximum power. For the first calculations the worst-case scenario for the Sun incidence angle was used, but later on in order to get more accurate values of our estimations a mid-point between these two cases, 8.16° was considered as the incidence angle.

Once both the beginning-of-life and end-of-life power have been established, the total power that the solar array must provide during daylight can be determined using

$$P_{sa} = \frac{\frac{P_e T_e}{X_e} + \frac{P_d T_d}{X_d}}{T_d} \quad (4.16)$$

where P_e and P_d are the satellite's power requirements during eclipse and daylight, and T_e and T_d are the lengths of these periods per orbit. X_e and X_d are the efficiency of the paths from the battery to the individual loads and the path directly from the arrays to the loads, respectively. [9]

Once both the total power that the solar array must provide, P_{sa} , Equation 4.16 and the end-of-life power, P_{EOL} , Equation 4.13, have been established, it is possible to obtain the solar array area, A_{sa} , that will be needed for the mission, Equation 4.12.

4.7.1.1 Solar cells selection

Due to the demanding power requirements of this mission, cells with a high level of efficiency must be selected. The two types of cells with a flight history are silicon cells and gallium arsenide cells, which are a more recent development. Since gallium arsenide cells have higher levels of efficiency, the Azure Space GaAs cells have been the ones selected, their main specifications can be consulted on Table 4.33 .

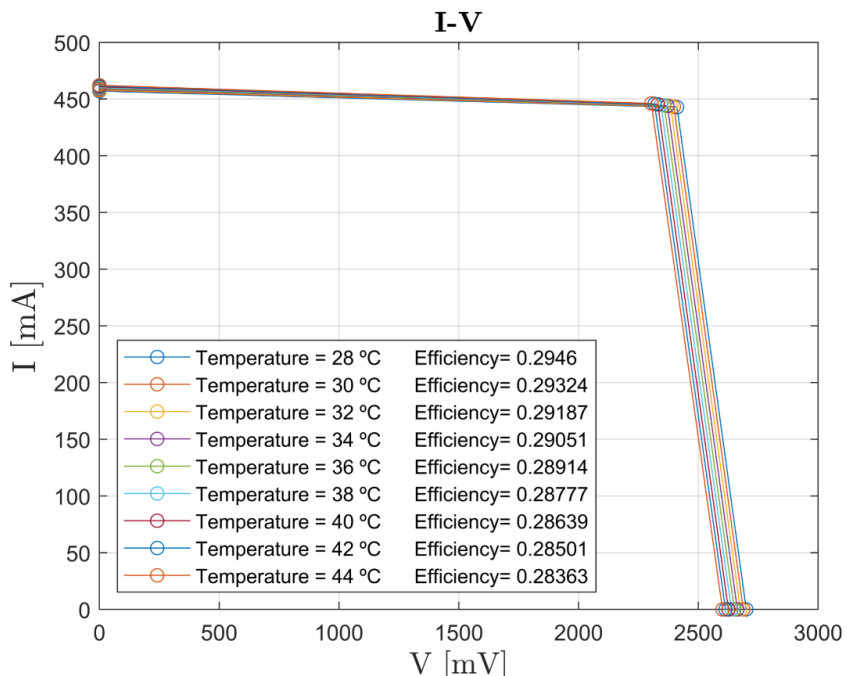
Table 4.33: Solar cell specifications.[28]

Base material	GaAs	Average Open Circuit V_{oc}	2700 mV
Dimensions	39.55 x 68.98 mm \pm 0.05 mm	Average Short Circuit I_{sc}	457.0 mA
Cell Area	26.51 cm ²	Voltage at max. Power V_{mp}	2411 mV
Cell Thickness	150 \pm 20 μ m	Current at max. Power I_{mp}	442.8 mA
Average Weight	\leq 2.35 g	Open Circuit Voltage	- 6.2 mV/ $^{\circ}$ C
Flight heritage	Since 2013	Short Circuit Current	0.32 mA/ $^{\circ}$ C
		Voltage at max. Power	- 6.7 mV/ $^{\circ}$ C
		Current at max. Power	0.21 mA/ $^{\circ}$ C

Although the value of the efficiency will vary with temperature, Figure 4.23b, since this is a preliminary stage of the design, for the following estimations it has been considered that the solar cells have a constant efficiency of 28.67%, which is the one associated to a 39.5 $^{\circ}$ C temperature, that has been estimated by the thermal subsystem to be the estimated temperature at which the solar panels are.



(a) AzurSpace 30% Triple Junction GaAs Solar Cell [28]



(b) I-V approximate profile of solar cells with temperature.

Figure 4.23: Solar Cell

This solar cells are used on ISISPACE Solar Panels [29]. ISISPACE offers customized CubeSat solar panels, supporting body mounted panels and deployable arrays for 1U to 12U sizes. After studying different possible configurations (see Section 4.7.5.1) the selected panels for this mission consist of body mounted panels on the 6U side of the satellite facing the sun and two deployable 3U panels from both the adjacent sides.

4.7.2 Energy Storage

A system for storing energy for peak-power demands and eclipse periods is also required. This system is typically a battery which consists of individual cells connected in series. The number of these cells is determined by the bus-voltage, and the amount of energy stored within the battery is the capacity. Batteries can also be connected in series to increase the voltage or in parallel to increase the current if it is required. The total capacity of the battery, C_r , is given by

$$C_r = \frac{P_e \cdot T_e}{DoD \cdot N \cdot X_e} \quad (4.17)$$

where P_e , T_e and X_e have already been defined, DoD is the depth of discharge, which is the percentage of total battery capacity consumed during a discharge period, and N is the number of non-redundant batteries. In this particular mission there are no eclipse periods, but as it will be analysed on Section 4.7.5.1, due to the high power requirements in certain operating modes the battery will need to provide power along with the solar panels. Once the total capacity of the battery is estimated, it is possible to select a suitable battery for the mission.

4.7.2.1 Battery Selection

After analysing different EPS configurations for this mission, a battery with a total capacity of 45Wh has been selected. An in-depth analysis of how this capacity has been estimated can be consulted in Section 4.7.5.1. This battery consists of a 4 cell Lithium-Ion mounted in series. The four cells are part of electrical component selected: the ISIS Electrical Power System [30] (Figure 4.24). The battery cell nominal voltage is 3.6 V, and battery cell nominal capacity 3200 mAh. Due to the fact that the ISIS EPS is a modular component, in case of any changes on the power system requirement, the number of Lithium-Ion cell can be changed.

Table 4.34: Battery specifications. [30]

Mass	310 ± 5 g
Volume	96 x 92 x 15.95 mm
Operational temperature	-40 to +70 °C
Output voltage domains	VDO: 12.8-16 V (1 channel) VD1: 5 V (4 channels) VD2: 3.3 V (4 channels)
Maximum output current per channel for [VDO], [VD1] and [VD2]	2.5 A
Maximum input voltage	16 V
Maximum input current per channel	2 A
Static consumption	90 mW
Flight heritage	Since 2018



Figure 4.24: ISIS Type B Battery [30]

4.7.2.2 Battery charge-discharge process

The DoD (Deep Of Discharged) is typically between 20-40% for Li-Ion cells [26]. In this case a DoD of 35% has been selected for the battery sizing due to the mission short duration, so not many battery cycles are required. In addition, a battery discharge efficiency of 90% has been considered.

The battery capacity is sized so as it is capable of providing sufficient power to measure with two pairs of radiometers at the same time during an orbit. Moreover, it must also be taken into account that a sufficient amount of time exists between measurements in order to charge the battery. This requirement will be fulfilled for the MM-2 described in Section 4.1.5. For MM-1 and MM-3 it would only be possible to take measurements with one pair of

radiometers due to the short periods of time required between measurements.

Regarding the eclipse duration, it is necessary to take into consideration that for the whole mission time no eclipses will occur. The total mission time will depend on which measurement mode (MM-1, MM-2 or MM-3) is selected as well as the operating time of UCM3 μ PPT. However, short after the end of the mission time for MM-2, three consecutive eclipses will take place. The three eclipses occur within a time of 3 h 45' 3.19" being the minimum time between them 1h 23' 47.33" and the longest duration of the eclipse 1147.233 s. After analysing this duration and considering the satellite in a survival mode corresponding with the nominal mode 1, there would be enough time for recharging the battery between the three eclipses, not having any impact in the continuation of the satellite's life.

A battery charging efficiency of 60% has been considered to estimate the minimum time in nominal mode required to ensure that the battery is fully charged. The time needed to recharge the battery after operating two pairs of radiometers at the same time during an orbit is 1.58 h.

4.7.3 Power Distribution, Regulation and Control

Regarding the power distribution from the solar panels to the different loads of the satellite as well as from the solar panels to the battery for recharging it, losses associated to the wires have been considered, giving them a value of 80% and 60% respectively.

The power subsystem may also need to convert and regulate voltage levels or supply multiple voltage levels. It frequently switches equipment on or off and, for increased reliability, protects against short circuits and isolates faults. [26]

Therefore, it is also necessary to consider that the EPS subsystem also has a PCU. The ISIS Modular Electrical Power System (Figure 4.24) include, the battery pack (4 cell Lithium-Ion), the Power Conditioning Unit (PCU) and the Power Distribution Unit (PDU).

The Power Conditioning Unit has 3-channel-MPPT (Maximum Power Point Tracker). The MPPT allows the panels to operate on the maximum power point. The solar panels interface delivery power to both the battery segment and the satellite segment. In addition, the battery segment included protection against short circuits, and the battery can be disconnected if needed [30].

The Power Distribution Unit can provided a regulated bus with four 3.3 V and 5V switchable outputs as well as an unregulated bus channel (12.8-16V). The values of the regulated bus from other similar missions such as ASTERIA or CubeSTAR have been considered in order to have an idea of typical regulated bus values.

Table 4.35: Subsystems power and voltage requirements.

Subsystem	Power requirement [W]	Voltage requirement [V]
Payload	10-30	-
ACDS	3.9	3.3/5/12
Communication	6.5	5
Data handling	0.4	3.3
Thermal	0	0
EPS	0.09	3.5
Structure	0	0

4.7.4 Estimating Total Power Requirement

Since this mission does not fall under any of the categories that have a power estimating relationship based on the power consumed by the payload [11], the estimation of the total power requirement has been done by estimating the power associated to each of the subsystems of the mission. Before doing this first power budget, it is necessary to define the different operating modes of this particular mission, which will differ in power requirements.

4.7.4.1 Operating modes

The spacecrafts tend to have several operating modes that differ in power requirements. It is necessary to budget separately each mode in order to find the most restrictive one. Since it is being tried to elaborate a reliable power budget, the operating mode which has the highest power requirement will be the one used to escalate the solar panels and battery that will be later selected. The importance of having a reliable power estimation is to make sure that the initial estimation of solar panel size is adequate. Due to the fact that the solar panels are normally long-lead items, problems regarding the panel delivery schedule, as well as substantial unplanned costs, will result if their size is initially underestimated and needs to be later increased. This explains the importance given to this initial estimation.

The nominal mode considers the power requirement of the on board computer, as well as the consumption of the thermal and electrical power subsystems. Although there could be some variations, since this is a preliminary estimation, it has been considered that the nominal mode also includes the whole consumption associated to the ACDS subsystem.

Table 4.36: Operating modes for the mission.

	Mode 1 (Nominal)	Mode 2	Mode 3	Mode 4	Mode 5	Mode 6
ACDS	✓	✓	✓	✓	✓	✓
Thermal	✓	✓	✓	✓	✓	✓
Data Handling	✓	✓	✓	✓	✓	✓
EPS	✓	✓	✓	✓	✓	✓
Communication		✓				
1-pair-radiometers			✓			
2-pair-radiometers				✓		
3-pair-radiometers					✓	
UCM3 μ PPT						✓

4.7.5 EPS Configuration Analysis

4.7.5.1 Sizing 6U-CubeSat Power Subsystem

To estimate the power budget, as well as to select the different components of the electrical power subsystem, it is necessary to continuously update the mission parameters. With the objective of illustrating the influence of the parameters, as well as showing the evolution of the power subsystem, the first and last estimation made during the development of the power subsystem will be explained, as well as the decisions taken in the process. Listed below are the main characteristics of these stages of development:

- **I1 (Initial Estimation)** : Definition of the operating modes and estimation of the power consumption of each subsystem based on typical power consumption in other mission. The parameters of the mission are not known in detail. Research and documentation on solar cells and batteries used in CubeSat.

- **I2 (Final Estimation)**: The mission parameters as well as the maximum power consumption of each subsystem are accurately defined.

• I1- Initial Estimation

The first step in the preliminary estimation of the power consumption, involved the study of the different operational modes covered in the section 4.7.4.1. However, initially, the only power values available corresponded to the payloads (Table 4.37).

Table 4.37: Payload Power Consumption

Payload	Power Consumption[W]
1-Pair Radiometer	10
UCM3 μ PPT	20

The first approximation of power consumption as a function of the operating mode is based on the estimation of the Table 4.38 , which shows the typical power consumption for each subsystem for a mission with a payload that consumes less than 100W [26].

Table 4.38: Typical power consumption by subsystem for small satellites (less than 100 W)[26]

Payload	20-50 W	Thermal	0 W
Attitude Control	0 W	EPS	10-30 W
Communication	15 W	Structure	0 W
Data Handling	5 W	Propulsion	0 W

Because this mission is not framed within one of the typical mission types such as a communications or meteorological mission, the values listed in Table 4.38, along with the analysis of some similar CubeSat missions, are a good starting point to bound the power requirements of each mode, in order to determine if there is enough area for the amount of solar cells required [26].

The Table 4.39a shows the preliminary maximum power values selected for each subsystem to calculate P_n and P_e values from equation 4.16. Power consumption for the payload has been fixed between 10-30W, corresponding to the use of 1,2 or 3 pairs of radiometers or UCM3 μ PPT. For communications and Data Handling subsystems, the default values shown in Table 4.38 have been assumed. However, for the power subsystem, it has been selected the value of 1W, instead of the one proposed in Table 4.38. This decision has been made due to the fact that the value shown in Table 4.38 takes into account the conversion and the line losses. However, P_n and P_e do not take into account the regulation and battery charging losses. Therefore, the consumption of 1W would be associated to the PCU.

Table 4.39: POWER BUDGET (I1)

(a) Power Subsystem requirement		(b) Power mode requirement	
Subsystem	Power Requirement	Power Requirement	Power Requirement
Payload	10-30 W	Mode 1	6 W
Attitude Control	0 W	Mode 2	21 W
Communication	15 W	Mode 3	16 W
Data Handling	5 W	Mode 4	26 W
Thermal	0 W	Mode 5	36 W
Power	1 W	Mode 6	26 W
Structure	0 W		

The parameters established in Table 4.44b, and discussed in section 4.7.1, will remain constant throughout the successive estimations. However, the values shown in Table 4.44a will be updated according to the changes in the mission parameters for each subsystem. Initially, there was only an estimation of how long the orbital period would be ($T_{orbital} = 5566.68$ s), as well as the maximum duration of the eclipse ($T_{eclipse} = 1121.935$ s).

At this point, it was unknown how long the communications mode will operate or whether it will be possible to take different measurements per day. However, starting from the objective of measuring and communicating at least once a day, and considering that an eclipse could take place that day, the required panel surface area was calculated in order to be able to supply the required power at the end of the mission. To do this, the average value of the power during the day was used as a value of P_n .

Table 4.40: Applied parameters (I1)

(a) Trade-of parameter.		(b) Constant parameter.	
η_p ($T = 28^{\circ}\text{C}$, 1637 W/m^2) [%]	29.5	Id	0.77
t_f [days]	365	c	0.0275
θ [$^{\circ}$]	8.16	P_{sun} [W/m^2]	1367
T_e [s]	1121.935	Cell Area [m^2]	0.002651
T_d [s]	85278	X_d	0.8
		X_e	0.6

The Table 4.41a shows the panel area required for the solar panels to provide sufficient power for modes 4, 5 and 6 taking into account losses. In Table 4.41b, it shows the necessary panel area from the estimated P_{sa} value. To get this value, one day has been taken as reference period, along with the average power of each one of the modes operating that day (nominal, communication, radiometers) in the case of measuring with two pairs of radiometers (mode 4) at the same time or with 3 pairs of radiometers at the same time (mode 6). N_{sa} is the number of solar cells based on the area of the chosen solar cell (Figure 4.23).

Table 4.41: Number of Solar Array (I1)

(a) Panel area with solar panels as the sole power source.			(b) Solar Array Power and Area Estimation		
	P/X_d [W]	A_{sa} [m^2]		P_{sa} [W]	A_{sa} [m^2]
Mode 4/6	32.5	0.1087	41	22.22	0.0743
Mode 5	45	0.15	58	26.38	0.0883

From these results, it can be concluded that:

-If the battery is not used, the area needed to measure with multiple pairs of radiometers operating at the same time is too large (Table 4.41a).

- The value of the power supplied by the panels during the daylight for the whole mission (P_{sa}) (Table 4.41b) is below the power required for each mode, therefore, it will be necessary to use the batteries during the day.

- In addition, the difference between P_{sa} and the power required for mode 5 is so significant that even if it was possible to recharge the battery during this period, it would result in the need of a very large battery capacity. Therefore, it will be considered at this stage that it will not be possible to operate using three radiometers at the same time.

In the successive stages of the design process of the electric power subsystem, the values of each subsystems were updated, studying the feasibility of each operational mode. For this purpose, different batteries and deployable panels configurations were taken into account.

• I2- Final Estimation

In this last stage, the operating temperature of the panel, the time of the mission, the maximum power consumed by each subsystem, as well as the operating time of each mode are known. For the subsequent calculations, the two typical commercial battery capacities for CubeSat, as well as two different configurations for the two deployable solar panels were taken into account (Table 4.42).

Table 4.42: EPS possible configurations

(a) Batteries capacities		(b) Deployable solar panels configuration	
	Capacity [Wh]		Number of solar cell
B1 (2 cell)	22	C1	26
B2 (4 cell)	45	C2	34

In order to decide how many single solar cells would fit according to size, it has been recurred to the customise options that the manufacturer provided, in which for an area of 6U (600cm²) the maximum number of cells is 14 and for an area of 3U (300cm²), the maximum number of cells is 6. C1 configuration corresponds to a fixed area of 6U and two deployable panels of 3U area. On the other hand, C2 configuration corresponds to a fixed area of 3U and two deployable panels of 6U area.

The measurement time required a mission duration of 90 days (measuring and communicating twice a day). However, a final time of 100 days has been implemented because after the phase of taking measurements with the radiometers, it is necessary to test UCM3 μ PPT during the final phase of the mission. This value is only representative, since there is no operating time requirement for UCM3 μ PPT.

In order to estimate the capacity of the battery that would allow to measure with two pairs of radiometers at the same time during a complete orbit, the following calculations have been made for the different combinations of batteries and solar panels:

- Calculation of the power that can supply the panel at the end of the mission.
- Calculation of the power that reaches the payloads after removing the losses (Xd)
- Calculation of the power that the battery has to supply for the corresponding mode.
- Calculation of the battery capacity.
- Calculation of the power available for charging the battery depending on the operating mode.

Table 4.43: POWER BUDGET (I2)

(a) Power Subsystem requirement		(b) Power mode requirement	
Subsystem	Power Requirement		Power Requirement
Payload	10-30 W	Mode 1 (Nominal)	4.39 W
Attitude Control	3.9 W	Mode 2	10.89 W
Communication	6.5 W	Mode 3	14.39 W
Data Handling	0.4 W	Mode 4	24.39 W
Thermal	0 W	Mode 5	34.39 W
Power	0.09 W	Mode 6	24.39W
Structure	0 W		

Table 4.44: Applied parameters (I2)

(a) Updated parameter		(b) Constant parameter.	
η_p ($T = 39.5^{\circ}\text{C}$, 1637 W/m^2)[%]	28.67	Id	0.77
t_f [days]	90+10	c	0.0275
θ [$^{\circ}$]	8.16	P_{sun} [W/m^2]	1367
		Cell Area [m^2]	0.002651
		X_d	0.8
		X_e	0.6

As it can be seen in Table 4.45a, for both configurations, the solar panels are able to supply the power required for operating modes 1, 2, 3. Therefore, it will be calculated, the power capacity required for modes 4, 6 and 5 since they are the most restrictive ones. As there is no time requirement for UCM3 μ PPT, it has been decided to set the battery capacity limits for mode 4, with the UCM3 μ PPT operating a time restricted to the battery capacity and the selected operating parameters.

Table 4.45: Solar panel power and batteries capacities

(a) Solar panel power.		(b) Minimum Battery capacity (DoD = 35%, n=0.9)	
	$P_{panel}[\text{W}]$	$P_{panel}/\text{Xd} [\text{W}]$	Battery Capacity (C1)[Wh]
C1	20.31	16.25	42.6
C2	26.56	21.25	91.8
			Battery Capacity (C2)[Wh]
Mode 4			14.8
Mode 5			64

It can be observed from Table 4.45a that the mode 5, as concluded at the beginning of the study of the subsystem, requires too much power supply. Therefore, it has been determined that the system cannot operate in this mode.

Moreover, in order to be able to decide which panel configuration is the most appropriate, it has been studied the effects of each of the configurations in the other subsystems specially in the thermal one. In addition to this, it has also been taken into account the consequences in the operating modes if one or both of the deployable panels fails. For both cases, this failure would mean that it would not be possible to operate with two pairs of radiometers at the same time. However, for the C1 configuration with the B2 battery, the time that the UCM3 μ PPT could operate is longer, so this configuration was finally chosen. Option C2-B2 was not considered, since the power system was being over-dimensioned.

In addition, when it comes to selecting the combination of cells in series and in parallel, it is necessary to take into account maximum input current per channel and maximum input voltage specified in Table 4.34 as well as the minimum input voltage to start MTTP (3.5V) from the ISIS EPS.

Because the possible combinations of the 26 solar cells originally selected result in voltage and current values not desired, it has been decided to eliminate one of the cells. The result is a solar panel with 25 solar cells. The final configuration is formed by 5 cells in series and 5 cells in parallel resulting in voltage and current values at the maximum power point, at a temperature of 28° C and an irradiance of 1367 W/m² of $V_{mp} = 12.005$ V and $I_{mp} = 2.21$ A.

4.8 Launcher Selection

The launcher selection process, which is part of the Mission Analysis subsystem, usually receives inputs from all the other subsystems and it is commonly started by the time there is a preliminary design idea of how the satellite is going to look like. This process usually takes five steps:

1. Requirement collection & Strategy deployment.
 - Number of satellites per launch
 - W_{dry}
 - Size
 - Mission orbit
 - Mission timeline
2. Identify and analyze acceptable configurations for the launch system.
 - $W_{propellant}$
 - $W_{adaptor}$
 - $W_{insertion}$
3. Potential launcher preliminary selection for spacecraft design.

The launcher manufacturer must set a competitive scenario on the next parameters:

- Cost
- Availability
- Reliability
- Ability to carry out the mission
- Launch conditions
- Commercial agreement

4. Determine spacecraft envelope inside the launcher.

- Fairing size and shape
- Loads
- Spacecraft environment (cleanliness, temperature...)
- Interfaces

5. Iterate to meet constraints.

For the launcher proposal it has been considered that it must satisfy the following conditions, based on the standard selection process:

- Able to put the spacecraft into a Sun-Synchronous RGT orbit :

$$i = 97.4 \pm i_{\text{injacc}} \quad h = 500 \text{ km} \pm h_{\text{injacc}}$$

- The launcher must leave the satellite in the final orbit because of the lack of any propulsion system
- The launcher must have a reliability of, at least, $R=0.9$
- The launcher must be able to perform multi-launch.
- The latitude of the launchpad will not be a problem due to inclination of the orbit selected.

Considering this criteria, there are two candidates for this launch.

1. Electron Rocket from Rocket Lab (American Private Space firm)
2. Soyuz from RKK Energiya (Russian Launch Manufacturer)

4.8.1 Electron

The Electron is a two-stage orbital launch vehicle developed by Rocket Lab. Electron was developed to offer a reliable injection in orbit for small satellites. Its typical mission implies putting several small satellites at once into a 500 km altitude SSO, therefore, it covers exactly the necessities of the Martin Lara mission. Its payload mass capacity for these type of missions is of 150 kg .

Most representative parameters of the launcher and the launch facilities are shown in the tables and graphs bellow.

Table 4.46: Electron's launch sites

Launch Site	Latitude	Longitude	SSO injection capability
Mahia, New Zealand	$\phi = 39.262^\circ S$	$\lambda = 177.865^\circ E$	YES
Wallops Island, Virginia, USA	$\phi = 37.834^\circ N$	$\lambda = 75.488^\circ W$	NO

Table 4.47: Electron's Reliability and Cost

Cost	$40000 \frac{\text{€}}{\text{kg}}$
Reliability	$R = 0.94$

Concerning to the loads that the payload would suffer during the launch campaign, the most representative ones are included in the appendix D.

Table 4.48: Injection accuracy for 500 km SSO.

Inclination	$\pm 0.15^\circ$
Altitude	$\pm 15\text{km}$

4.8.2 Soyuz

Soyuz rockets represents a soviet rocket family built of four stages in total. In the Figure 4.25 are included a representative scheme of one of Soyuz's configurations.

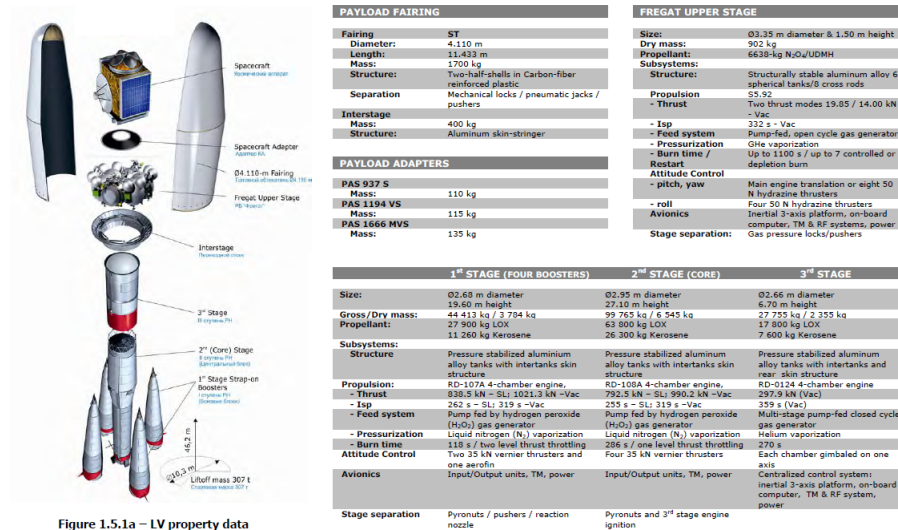


Figure 4.25: Soyuz propulsion system configuration

The most representative parameters from this launcher are detailed tables bellow.

Table 4.49: Soyuz's launch sites

Launch Site	Latitude	Longitude
Baikonur Cosmodrome	$\phi = 45.965^\circ N$	$\lambda = 63.305^\circ E$
Plesetsk Cosmodrome	$\phi = 62.925^\circ N$	$\lambda = 40.578^\circ E$
Vostochny Cosmodrome	$\phi = 51.885^\circ N$	$\lambda = 128.335^\circ E$
Kourou Cosmodrome	$\phi = 5.184^\circ N$	$\lambda = 52.763^\circ W$

Table 4.50: Soyuz's Reliability and Cost

Cost	$5357 \frac{\$}{kg}$
Reliability	$R = 0.97$

Table 4.51: Injection accuracy for 500 km SSO.

Inclination	$\pm 0.12^\circ$
Altitude	$\pm 12\text{km}$

Regarding the loads that the payload would suffer during the launch campaign, the most representative ones are included in the appendix D.

5. Risk Analysis

The scoring schemes applied to assess the severity and likelihood of each risk are those of the ECSS standards [31]. These can be found in Tables C.1 and C.2 in Appendix C.

Once the risk management policy is established, the risks of MARTINLARA mission will be identified and assessed. The naming convention applied to identify each risk will follow the structure **Subsystem-Enumeration**.

Table 5.1: Risks naming convention

Code	Description		
Subsystem	Risk type regarding the subsystem involved (MA, ADCS, TH, PS, ST, CM)		
Enumeration	Identifying number of the risk within the subsystem (XXX)		

5.1 Structure

Project ID: MARTILARA		Organization: MARTINLARA Consortium		
Risk	Impact between solar panel and dispenser			ID: ST-001
	Severity	Likelihood	Risk index	Risk domain
	5	C	HIGH	Structure
Causes and consequences	The bad positioning of the bearings on the 3U panels can cause that during the ejection of the satellite the panels impact the dispenser, leaving it with no power.			
Risk reduction measures	To reduce this risk, it is proposed to carry out numerical simulations and tests with different bearing positions to reduce the probability of impact.			
	Accepted risk	<input type="checkbox"/>	Reduced risk	<input checked="" type="checkbox"/>

Project ID: MARTILARA		Organization: MARTINLARA Consortium		
Risk	Permanent deformation Zenit sheet			ID: ST-002
	Severity	Likelihood	Risk index	Risk domain
	4	C	MEDIUM	Structure
Causes and consequences	Zenit radiometers have the most restrictive FOV and there is a risk that the covering sheet will deform during launch due to vibrations.			
Risk reduction measures	To reduce this risk, it is proposed to carry out a FEM study looking for the plate's own frequencies. If any of them is close to the one transmitted by the dispenser, the structure must be modified to increase its rigidity.			
	Accepted risk	<input type="checkbox"/>	Reduced risk	<input checked="" type="checkbox"/>

5.2 Thermal Control

Project ID: MARTILARA			Organization: MARTINLARA Consortium				
Risk	Insufficient accuracy of the model			ID: TH-001			
	Severity	Likelihood	Risk index	Risk domain			
	3	C	LOW	Thermal Control			
Causes and consequences	Inaccuracy of the current thermal model could lead to temperature ranges, greater than the survival and operational temperatures of the equipment, damaging it.						
Risk reduction measures	Use of certified programs such as ESATAN-TMS to reduce inaccuracy.						
	Accepted risk	<input type="checkbox"/>	Reduced risk	<input type="checkbox"/>			

Project ID: MARTILARA			Organization: MARTINLARA Consortium				
Risk	Miscalculation of orbit			ID: TH-002			
	Severity	Likelihood	Risk index	Risk domain			
	5	A	LOW	Thermal Control			
Causes and consequences	Miscalculation of eclipse duration or orbit perturbation, when defining the orbit, could lead to temperatures outside the survival range of some instruments, causing a major failure in the satellite.						
Risk reduction measures	Implementing a more complex thermal model that accounts for transitory temperature during the on-orbit life, taking into account the orbit decay and eclipse periods.						
	Accepted risk	<input type="checkbox"/>	Reduced risk	<input type="checkbox"/>			

5.3 Attitude Determination and Control

Project ID: MARTILARA			Organization: MARTINLARA Consortium				
Risk	Long-term failure of the ADCS			ID: AD-001			
	Severity	Likelihood	Risk index	Risk domain			
	5	B	MEDIUM	Attitude Determination and Control			
Causes and consequences	Failure of the ADCS results in the sun hitting the science instruments during measurements. Critical, as it could end or partially affect the mission.						
Risk reduction measures	The use of several sensors for attitude determination is encouraged in order to increase the satellite's knowledge of the surroundings.						
	Accepted risk	<input type="checkbox"/>	Reduced risk	<input checked="" type="checkbox"/>			

Project ID: MARTILARA			Organization: MARTINLARA Consortium				
Risk	Reaction Wheels becoming saturated			ID: AD-002			
	Severity	Likelihood	Risk index	Risk domain			
	4	C	MEDIUM	Attitude Determination and Control			
Causes and consequences	Reaction Wheels becoming saturated during science measurements could cause a loss of attitude control and result in a missing a window opportunity for the science observations.						
Risk reduction measures	A secondary actuator system will be implemented to be used when the reaction wheels become saturated. Furthermore, software will be used to monitor and prevent the saturation of the wheels.						
	Accepted risk	<input type="checkbox"/>	Reduced risk	<input checked="" type="checkbox"/>			

5.4 Command and Data Handling

Project ID: MARTILARA			Organization: MARTINLARA Consortium				
Risk	Memory Filling			ID: ST-001			
	Severity	Likelihood	Risk index	Risk domain			
	2	C	Low	Structure			
Causes and consequences	There is a risk that the stored data cannot be transmitted and the memory becomes full, with the consequent loss of information.						
Risk reduction measures	It is proposed to reduce the risk by increasing memory to ensure that the satellite can store data for a certain minimum time.						
	Accepted risk	<input type="checkbox"/>	Reduced risk	<input checked="" type="checkbox"/>			

5.5 Communication

Project ID: MARTILARA			Organization: MARTINLARA Consortium				
Risk	Malfunction of the transceiver			ID: CM-001			
	Severity	Likelihood	Risk index	Risk domain			
	5	A	LOW	Communication			
Causes and consequences	Due to a technical or mechanical failure, the transceiver might stop receiving or transmitting data, or even both. This fact will lead to the failure of the mission.						
Risk reduction measures	The only way to reduce this risk would be to include more than one transceiver onboard. However, based on CubeSat's standards, only one transceiver can be placed on the satellite.						
	Accepted risk	<input checked="" type="checkbox"/>	Reduced risk	<input type="checkbox"/>			

Project ID: MARTILARA			Organization: MARTINLARA Consortium				
Risk	Malfunction of the antenna			ID: CM-002			
	Severity	Likelihood	Risk index	Risk domain			
	5	A	LOW	Communication			
Causes and consequences	The failure of the antenna would entail the complete failure of the mission, since it is not possible to communicate the measured data without this instrument.						
Risk reduction measures	Placement of one redundant antenna, which operates with a deployable system. It is necessary to consider that this solution would imply an extra power consumption during its deployment.						
	Accepted risk	<input checked="" type="checkbox"/>	Reduced risk	<input type="checkbox"/>			

Project ID: MARTILARA			Organization: MARTINLARA Consortium				
Risk	Lost contact with the ground station			ID: CM-003			
	Severity	Likelihood	Risk index	Risk domain			
	5	A	LOW	Communication			
Causes and consequences	If the final orientation of the satellite is not the required, it might cause the lost of contact with the ground station, impeding the satellite communication.						
Risk reduction measures	Consider the different orientations the satellite might have and choose more than one ground station that will be able to contact with the satellite with those orientations.						
	Accepted risk	<input checked="" type="checkbox"/>	Reduced risk	<input type="checkbox"/>			

5.6 Electric Power Subsystem (EPS)

Project ID: MARTILARA			Organization: MARTINLARA Consortium				
Risk	Solar panels deployment failure			ID: PW-001			
	Severity	Likelihood	Risk index	Risk domain			
	4	C	MEDIUM	EPS			
Causes and consequences	The solar panels of this mission occupy the surface of the 6U satellite's face as well as the two 3U adjacent satellite faces which are in orbit deployed. The malfunction of the panels' mechanism can cause failures in the deployment of these two 3U solar panels.						
Risk reduction measures	To mitigate this, along with exhaustive structural analysis, the panels have not been placed in any critical surface for the mission. The EPS configuration has also been selected to allow the mission to continue without deployed panels in the operating mode 3.						
	Accepted risk	<input type="checkbox"/>	Reduced risk	<input checked="" type="checkbox"/>			

Project ID: MARTILARA			Organization: MARTINLARA Consortium				
Risk	Electrical power distribution failure			ID: PW-002			
	Severity	Likelihood	Risk index	Risk domain			
	4	C	MEDIUM	EPS			
Causes and consequences	A primary regulated power bus is distributed to payload units. A failure in this distribution of power to the payload units can occur.						
Risk reduction measures	The PCU can switch equipment on or off and, protecting against short circuits and isolating faults. Which prevents failure propagation from one channel to the other.						
	Accepted risk	<input type="checkbox"/>	Reduced risk	<input checked="" type="checkbox"/>			

5.7 Launcher

Project ID: MARTILARA			Organization: MARTINLARA Consortium				
Risk	Launcher Failure			ID: PW-002			
	Severity	Likelihood	Risk index	Risk domain			
	5	C	High	EPS			
Causes and consequences	Failure in the launcher structure or being unable to deliver the satellite to the target orbit would lead to a mission loss.						
Risk reduction measures	Take out an insurance plan						
	Unresolved risk	<input checked="" type="checkbox"/>	Reduced risk	<input type="checkbox"/>			

6. Conclusions

To summarize the selected concepts and solutions for the proposed design, a brief résumé of each subsystem is presented below.

- For the **Mission Analysis**, the work started by developing the orbit initial proposal, which was done by the whole team. The characteristics of the mission lead to a quite low number of orbit options. Therefore once the decision of using a 500 Km SSO 6AM was taken, the process became iterative and started to generate a constant flow of inputs and outputs with the other subsystems. The work in mission analysis has been done trying always to meet not only the requirements but also the goals defined by the requirements. After all the iterative process, the orbit final proposal satisfies the other subsystems' specifications, meet the requirements and achieve some of the goals.
- For the **Structure System**, a COST 6U structure was selected as primary structure. To achieve compliance with the FOV of the radiometers, the covers and extensions have been machined, in addition to laser cutting the rest of the panels. With this solution the CubeSat standards and the dispenser requirements have been met.
- For the **Thermal Control System**, a three-node model was developed. The results obtained show that no active heating is required, reducing the necessary power for the satellite and reaching an internal optimal temperature via appropriate coatings. Without any certified tools as ESATAN-TMS this method provides sufficient data for this the preliminary design.
- For the **Attitude Determination and Control System**, the components were selected in order to provide the most appropriate solution for the mission requirements, while maintaining a low mass and power budget. These were then sized appropriately to counteract the estimated external disturbances.
- For the **Communication Subsystem**, Kiruna is the ground station selected, which is placed in an appropriate location and belongs to the core ESA network of ground stations. Regarding the antenna, it is a patch so it does not have any deployment system, minimising the failure risk which implies the mechanism and the power consumption. Finally, due to size restrictions, instead of having a receiver and a transmitter, the satellite will carry a transceiver.
- For the **Electric Power Subsystem** the configuration selected consists of a body mounted solar panel on the 6U side of the satellite facing the sun and two deployable 3U panels from both the adjacent sides. The solar panels consist of a total of 25 GaAs solar cells with an area per cell of 26.51 cm². The battery has been size to allow the goal of two pair of radiometers measuring on mission mode 2. A PCU and other regulators are also needed for peak power points.
- For the **Launcher Selection**, due to the low mass of the spacecraft, the principal objective was to find launchers capable of making a multiple launch and with high reliability. With this in mind, we make two different proposals, the Electron and the Soyuz. It has been decided that the one which better meets our necessities is the Electron due to its experience launching several CubeSats at once, and therefore it is the best option.

Regarding the Risk Analysis, the risks associated with each subsystem have been assessed. The pertinent decisions have been taken for each risk, for either actions during the design process or for future actions throughout the project development.

MISSION TYPE: Scientific/Technology demonstrator	
MASS 6,92 kg	DIMENSIONS CubeSat 6U Stowed for launch: 232x365x101mm Solar pannels deployed: 397x365x101mm
ORBIT	
Type of orbit: Circular Sun-synchronous orbit 6AM Altitude: 500 km Inclination: 97.406° Orbital Period: 5576 s t_{maxeclipse}: 0 s (During operation period) t_{mission}: 100 days Period of operation: From 2 nd March to 2 nd June Launch Date: 28 th February	
PAYLOADS	
Photonic payload: Including 3 Nadir antennas and 3 Zenith antennas, with an inclination of 15° on the Zenith face Micropropulsion System: Exterior opening in line with the COG Retro-reflector array: Positioned on Nadir	
COMMUNICATIONS	
Band: S-band Antenna: ISIS S-band patch antenna Transceiver: NanoAvionics CubeSat S-BandTransceiver Ground station: Kiruna (Sweden)	
ELECTRICAL POWER	
Solar array description: body mounted solar panel, using GaAs solar cells of 26.51 cm ² , on the 6U side of the satellite facing the sun and two deployable 3U panels from both the adjacent sides. Beginning of life power: 298.72 $\frac{W}{m^2}$ End of life power: 296.45 $\frac{W}{m^2}$ Battery description: Total capacity of 45 Wh consisting of four lithium-ion cells mounted in serie.	
ATTITUDE DETERMINATION AND CONTROL	
Attitude control method: 3-axis active control, zero momentum stabilisation. Attitude determination method: 3 axis attitude and position determination system. Sensors: Sun sensors, magnetometer, IMU and GPS. Actuators: Reaction wheels and magnetorquer.	
THERMAL CONTROL	
Active Heating: No active heating is required for this mission. Passive Solutions: Black, Kapton and Aluminized Kapton coatings in different faces.	

A. Appendix A: Requirements

Table A.1: Requirements of the MARTINLARA mission.

Requirement ID	Definition
R - 010	The S/C shall comply with the CubeSat standards.
R - 020	The S/C shall be a 6 units CubeSat maximum.
R - 030	The orbit altitude shall be 550 km as maximum.
R - 040	The orbital plane cannot contain the Earth-Sun radio-vector.
R - 050	Each pair of twin radiometers (Nadir and Zenith pointing) shall operate simultaneously for cross-calibration purposes (Goal: more than one pair).
R - 060	The radiometers shall take measurements with each radiometer pair for 2 orbits.
R - 070	The radiometers shall take measurements during 1 month (splitting this time among the three radiometer pairs) (Goal: Three months).
R - 080	Platform shall measure and keep, during operation, the external sides of the radiometers at an operational temperature range of 11-21°C, being 16°C the optimum temperature for operation. The survival temperature range is within -20°C to +50°C
R - 090	The radiometers Nadir antennas shall have a FOV (Field of View) of 60 deg (± 1 deg) half angle along its normal free of the Sun and spacecraft obstacles during operation.
R - 100	The radiometers Zenith antennas shall have a FOV of 90 deg (± 1 deg) half angle along its normal free of the Sun, Earth and spacecraft obstacles during operation.
R - 110	The Sun penetration in the FOV of each Nadir antenna shall be recorded as a function of time.
R - 120	The Sun and Earth penetration in the FOV of each Zenith antenna shall be recorded as a function of time.
R - 130	Measurements with each Nadir antenna shall be taken over a circular area of 500 km around the South (North) Magnetic Pole.
R - 140	Nadir antennas shall observe an Earth projected area (spot) of a maximum of 25 km of semi-major axis.
R - 150	Deviation from Nadir direction shall be, as a maximum, of +/- 5 deg during measurement.
R - 160	The 3-axis pointing accuracy of the satellite shall be of at least 1 deg (Goal: 0.1 deg).
R - 170	The 3-axis attitude determination shall be known with an accuracy of 0.1 deg with respect to Nadir (Goal: 0.05 deg).
R - 180	The absolute position of the spacecraft shall be determined with accuracy better than 10m RMS.
R - 190	Spacecraft shall carry and service the experimental UC3M- μ PPT.
R - 200	Spacecraft shall carry and service the retro-reflector system.

B. Appendix B: ADCS Perturbation Analysis

B.1 Gravity Gradient Torque

This torque derives from the fact that planetary gravitational fields decrease with the square of the radius from the centre of the planet according to the Newtonian law of gravitation. Hence, due to the finite distance between the opposite ends of the spacecraft, there is a slight variation in the forces acting on them. This differential results in a torque that tends to align its minimum inertia matrix (which is assumed to be the satellite's longitudinal axis) with the nadir-zenith direction. The gravity gradient torque for a satellite is defined by Equation B.1, where μ is Earth's gravitational parameter ($3.986 \cdot 10^{14} \text{ m}^3 / \text{s}^2$), r_p is the periapsis radius (6871m), I_{min} (0.032 kg.m²) and I_{max} (0.08 kg.m²) are the minimum and maximum moment of inertia respectively, and θ (0.1deg) is the maximum angular deviation between the longitudinal axis and the nadir-zenith direction.

$$T_g = \frac{3\mu}{r_p^3} |I_{max} - I_{min}| \sin(2\theta) \quad (\text{B.1})$$

Therefore, the estimated gravity gradient torque is $3.93 \cdot 10^{-10} \text{ N.m}$. It is interesting to note that the phenomenon of gravity gradient torque can be exploited for providing control stability to a spacecraft, as a passive attitude control method. [16]

B.2 Solar Radiation Pressure (SRP) Torque

The SRP torque is originated due to the difference in the location of the satellite's centre of pressure and its centre of mass. It is caused by the incident electromagnetic radiation which causes a pressure and a shear stress over the radiated surface. As the sun has the largest effect on this disturbance, the torque is cyclic for satellites that point at the Earth and it also shows an annual variation associated to the eccentricity of Earth's orbit. However, this also allows for the solar irradiance flux to be used to estimate the torque, which is mainly influenced by the spacecraft surface reflectivity coefficient and its geometry and by the position of the centre of gravity. Therefore, the torque is defined by:

$$T_{sp} = \frac{\phi}{c} A_{sp} (1 + q) \cos(i) \| \mathbf{c}_{sp} - \mathbf{c}_g \| \quad (\text{B.2})$$

For Equation B.2 the following parameters are considered: the solar flux, ϕ , which at Earth's orbit is around 1367 W/m^2 , c is the speed of light, the reflectivity coefficient of the satellite, q , which is taken to be at around 1, the sun light incident angle, i , which for MARTINLARA is 16.3265deg, the area that the SRP is incident to, A_{sp} , is 0.136 m^2 , and the centre of gravity, c_g , and the centre of solar pressure c_{sp} , are 0.167 m and 0.170 m respectively. The estimated SRP torque was $4.47 \cdot 10^{-9} \text{ N.m}$. [13]

B.3 Aerodynamic Drag Torque

In low earth orbits (LEO, < 2,000 km), the effect of Earth's atmosphere, or drag, must also be considered on the satellite's attitude. This effect is dominant for orbits below 500 km. It can be estimated by

$$T_a = \frac{1}{2} \rho_{atm,p} C_D A_a V_p^2 \| \mathbf{c}_p - \mathbf{c}_g \| \quad (\text{B.3})$$

where the atmospheric density at the periapsis, $\rho_{atm,p}$, is $7.30 \cdot 10^{-13} \text{ 4.47 kg/m}^3$ (using the MSISE-90 Model), the drag coefficient C_D , is usually taken to be at around 2 for similar satellites, the projected area in the velocity direction, A_a , is 136 m^2 , the satellite's velocity at the periapsis, V_p , is 7762.7 m/s , and the centre of gravity, c_g , and the centre of pressure c_p , are 0.167m and 0.0851m respectively. Therefore, using Equation B.3, the estimated torque is $2.19 \times 10^{-8} \text{ N.m}$. [15]

B.4 Magnetic Torque

This torque results from the interaction between the residual magnetic dipole of the spacecraft and the magnetic field of the Earth. The former is a factor to be minimised during the final design phases of the satellite but it will not

be null. Furthermore, it can only be measured through testing, and hence, the issue lies in that the MARTINLARA CubeSat is still in the mission design phase so an estimate will be used until more accurate data is obtained. It was found that typical values are in the range of 0.2 to 20 Am^2 , however, those values concern larger spacecraft so a value for a 6U Cubesat still had to be found. According to some sources, a value of 0.2 Am^2 for the residual magnetic dipole, D_m , seems to be a safe guess for a 6U CubeSat. Thus, the residual magnetic dipole torque can be estimated by

$$T_m \approx D_m \frac{\lambda M_m}{r_p^3} \quad (\text{B.4})$$

where the magnetic moment of the Earth, M_m , is $7.96 \cdot 10^{15} T.m^3$, r_p is the periapsis radius, and the unit-less function of the magnetic latitude, λ , which is taken to be 2 which corresponds to its value at the magnetic poles. [13]

C. Appendix C: Risk Assessment Criteria

Following the ECSS standards, the risk assessment criteria followed in this document is presented below. To begin with, risks are classified according to the severity of their consequences as shown in Table C.1.

Table C.1: Severity criteria.

Score	Severity	Severity of consequence
5	Catastrophic	Leads to termination of the project.
4	Critical	Unable to reach minimum success.
3	Major	Unable to reach partial success.
2	Significant	Unable to reach complete success.
1	Negligible	Minimal or no impact on the mission.

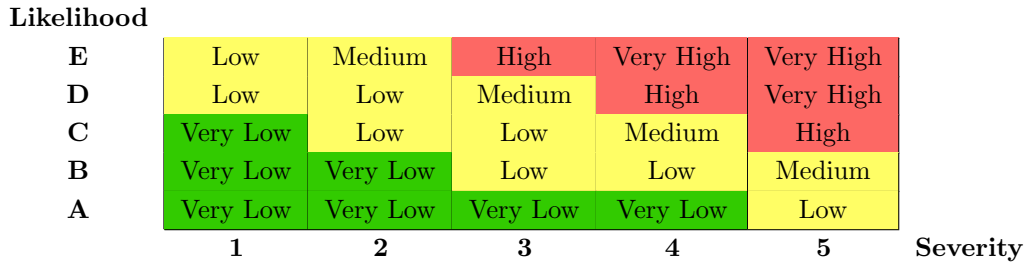
Additionally, the description of the levels of likelihood can be seen in Table C.2.

Table C.2: Risk level depending on the likelihood of occurrence

Level	Likelihood	Probability of occurrence
E	Maximun	Some phase of the project will surely happen
D	High	Happen frequently, 1 each 10 projects
C	Medium	Happen occasionally, 1 each 100 projects
B	Low	Happen rarely, 1 each 1000 projects
A	Minimum	hardly ever happen, 1 each 10000 or more projects

Hence, the risk index is established from the different combinations of severity and probability levels. Table C.3 illustrates the different risk indexes.

Table C.3: Risk index and magnitude scheme



Finally, the proposed actions and risk acceptance criteria to be applied according to the risk index established in Table C.3 can be seen in Table C.4.

Table C.4: Proposed actions for individual risks

Risk index	Risk magnitude	Proposed actions
E4, E5, D5	Very High risk	Unacceptable risk: implement new team process or change baseline – seek project management attention at appropriate high management level as defined in the risk management plan
E3, D4, C5	High risk	Unacceptable risk: see above.
E2, D3, C4, B5	Medium risk	Unacceptable risk: aggressively manage, consider alternative team process or baseline – seek attention at appropriate management level as defined in the risk management plan.
E1, D1, D2, C2, C3, B3, B4, A5	Low risk	Acceptable risk: control, monitor – seek responsible work package management attention.
C1, B1, A1, B2, A2, A3, A4	Very Low risk	Acceptable risk: see above.

D. Appendix D: Launcher loads

D.1 Electron

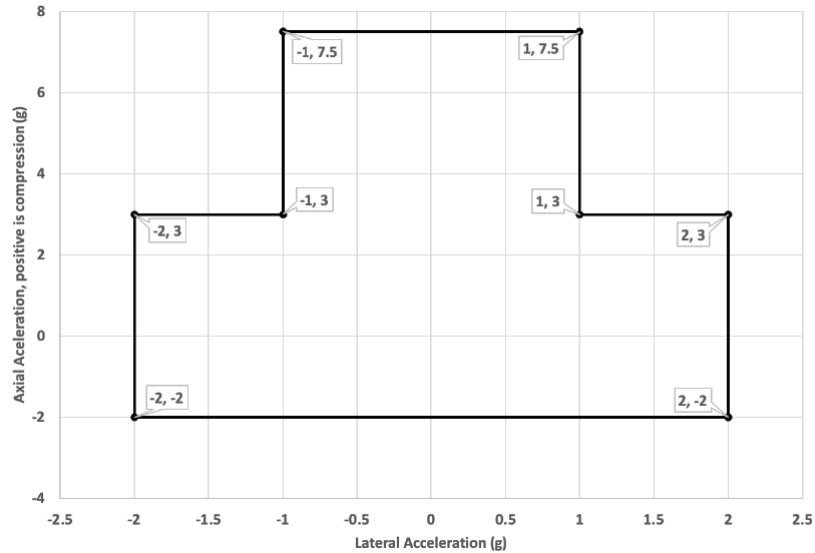


Figure D.1: Electron Acceleration MPE.

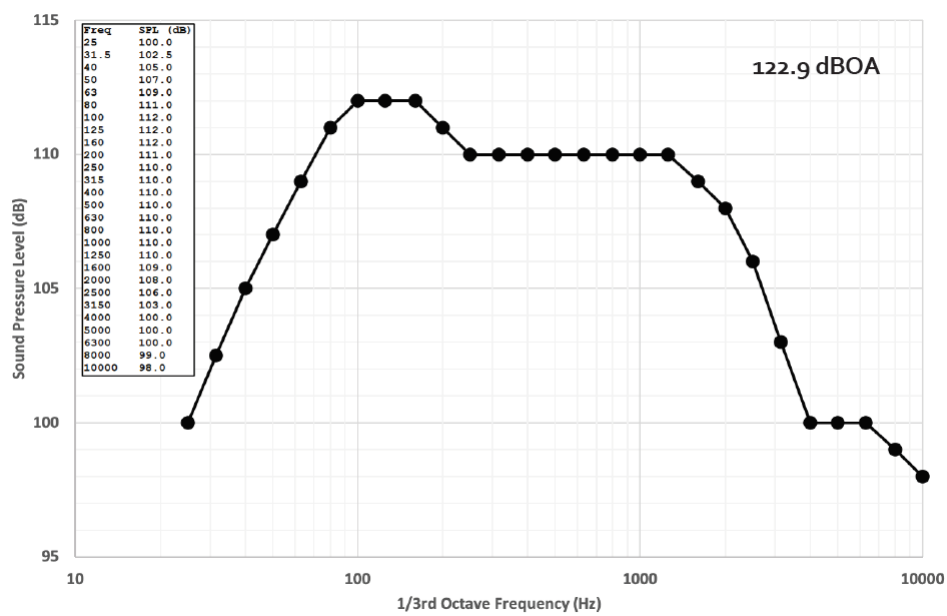


Figure D.2: Electron Acoustic MPE.

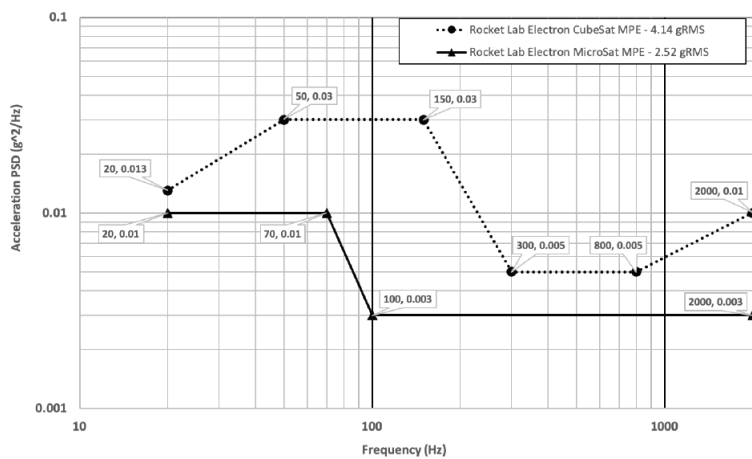


Figure D.3: Electron Random Vibration MPE.

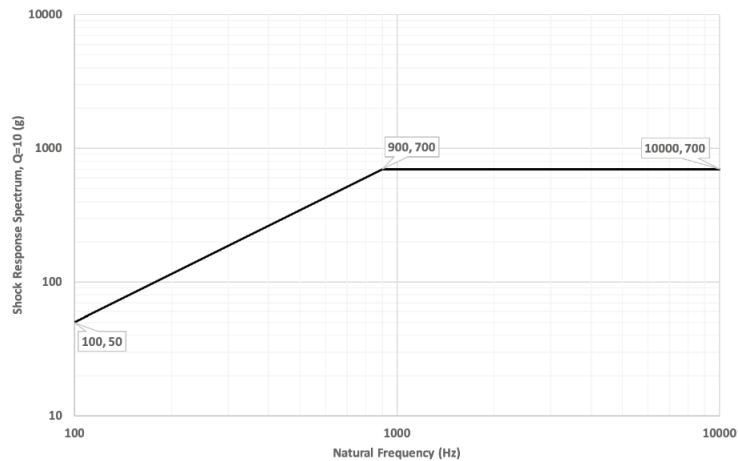


Figure D.4: Electron Shock MPE.

D.2 Soyuz

Octave Center Frequency (Hz)	Flight Limit Level (dB) (reference: 0 dB = 2×10^{-5} Pa)	
	filling factor $\leq 50\%$	50% < filling factor $\leq 70\%$
31.5	125	126
63	132	133
125	134	136
250	136	138
500	134	134
1000	125	125
2000	121	121
OASPL ⁽¹⁾ (20 – 2828 Hz)	140.5	141.9

Note ⁽¹⁾: OASPL – Overall Acoustic Sound Pressure Level

Figure D.5: Payload acoustic flight loads.

Octave Center Frequency (Hz)	ST-Type Fairing
	Flight Limit Level (dB) (reference: 0 dB = 2×10^{-5} Pa)
31.5	86
63	92
125	93
250	99
500	103
1000	107
2000	113
OASPL ⁽¹⁾ (20 – 2828 Hz)	118.3

Note ⁽¹⁾: OASPL – Overall Acoustic Sound Pressure Level

Figure D.6: Payload acoustic ground loads.

Load Event		QSL (g) (+ = tension; - = compression)					
		Lateral			Longitudinal		
		Static	Dynamic	Total	Static	Dynamic	Total
0	Ground transportation	-	± 0.3	± 0.3	-1.0	± 0.3	min -1.3 max -0.7
1	Lift-off	± 0.2	± 1.6	± 1.8	-1.0	± 0.6	min -1.6 max -0.4
2	Flight with maximum dynamic pressure (Qmax)	± 0.4	± 0.7	± 1.1	-2.4	± 0.4	min -2.8 max -2.0
3	First-stage flight with maximal acceleration	± 0.1	± 0.8	± 0.9	-4.3	± 0.7	min -5.0 max -3.6
4	Separation between first and second stages	± 0.2	± 0.9	± 1.1	-4.1	± 0.2	min -4.3 max -0.6
5	Second-stage flight	± 0.1	± 1.1	± 1.2	-1.0	± 0.4	min -4.0 max -0.6
6	Separation between second and third stages	± 0.2	± 0.6	± 0.8	-2.6	± 0.7	min -3.3 max +1.3
7	Beginning of third-stage flight	± 0.2	± 0.6	± 0.8	-1.0	± 1.9	min -2.9 max +0.9
8	Third-stage engine cutoff	± 0.1	± 0.3	± 0.4	-4.0	0.0	min -4.0 max +1.8

Figure D.7: Payload static and dynamic loads.

Flight Event	Frequency (Hz)		
	100–1000	1000–2000	2000–5000
	SRS, Shock Response Spectra (Q = 10) (g)		
Fairing & stages separations	15–350	350	350–200

Table 3.2.7a - Shock response spectra at Fairing and stages separations

Spacecraft Adapter Interface Diameter	Frequency (Hz)		
	100–1000	1000–10000	
	SRS, Shock Response Spectra (Q = 10) (g)		
$\varnothing 937$, $\varnothing 1194$, $\varnothing 1666$	20–1000	1000–700	

Table 3.2.7b - Shock response spectra for off-the-shelf clamp band separation systems

Figure D.8: Payload shock response.

Phase	Air conditioning system	Temperature [°C]	Relative humidity [%]	Air flow rate [Nm ³ /h]	Duration
Launch preparation nominal sequence					
01	Operation in S3B	S3B air conditioning system	17 ± 1°C	55 ± 5	-
02	Upper Composite transfer from S3B to ZLS	PFRCS air conditioning system	16 ± 1°C	55 ± 5	1500 ± 10%
03	UC hoisting to platform	Low flow rate to maintain a positive delta pressure under Fairing	Ambient temperature	Dew point ≤ -10°C	300 ± 10%
04	Removal of UC cover and beginning of UC mating on Soyuz three-stage	VSOTR	10 < T° < 25°C ± 1°C ⁽¹⁾	Dew point ≤ -10°C	1500 ± 10%
05	Finalization of UC mating on Soyuz three-stage	VSOTR	10 < T° < 25°C ± 1°C ⁽¹⁾	Dew point ≤ -10°C	4500 ± 10%
06	Integrated Launch Vehicle stand-by and launch preparation	VSOTR	10 < T° < 25°C ± 1°C ⁽¹⁾	Dew point ≤ -10°C	6000 ± 10% ⁽²⁾
07	Launch final count-down	STVVD	10 < T° < 25°C ± 2°C ⁽¹⁾	Dew point ≤ -55°C	1550 ± 10% ⁽²⁾
Aborted/reported launch sequence					
08	Aborted/reported launch sequence	STVVD	10 < T° < 25°C ± 2°C ⁽¹⁾	Dew point ≤ -55°C	1550 ± 10% ⁽²⁾
09	Integrated Launch Vehicle stand-by and launch preparation	VSOTR	10 < T° < 25°C ± 1°C ⁽¹⁾	Dew point ≤ -10°C	6000 ± 10% ⁽²⁾
					H0 → H0 + 2h30 →

Figure D.10: Payload thermal environment.

Event	Frequency Band (Hz)						Gage (g)	Duration of application (s)
	20 - 50	50 - 100	100 - 200	200 - 500	500 - 1000	1000 - 2000		
	PSD, Power Spectral Density ⁽¹⁾ (10^{-3} g ² /Hz)							
1 st stage flight	5.0 10.0	5.0 25.0	10.0 25.0	25.0 10.0	25.0 10.0	10.0 5.0	4.94	120
2 nd stage and 3 rd stage flight	2.5 5.0	2.5 10.0	5.0 10.0	10.0 5.0	10.0 2.5	5.0 1.0	3.31	480
Fregat flight	2.0	2.0	2.0	2.0	2.0 1.0	1.0	1.63	1100

Figure D.9: Payload random loads.